

ANALYSIS OF STATOR ACTIVE AND REACTIVE POWER IN A DOUBLY FED INDUCTION GENERATOR

A thesis is submitted to fulfil the requirement of the degree

Master in Electrical Engineering

Submitted by

KUNAL DUTTA

Examination Roll no. – **M4ELE23002**

Registration no. – **160164** of **2021-2022**

Year – **2nd**, Semester – **4th**

Under the Guidance of

Prof (Dr.) Debashis Chatterjee

Prof Nikhil Mondal

Prof Mihir Hembram

Department of Electrical Engineering

Jadavpur University

Kolkata – 700032

June 2023

**Faculty of Engineering and
Technology Jadavpur University,
Kolkata - 700032**

Certificate

This is to certify that the thesis entitled “**Analysis of Stator Active and Reactive Power in a Doubly fed Induction Generator**” submitted by **Kunal Dutta** (Examination Roll No: **M4ELE23002**), under our supervision and guidance during the session of 2021-23 in the department of Electrical Engineering, Jadavpur University. We are satisfied with his work, which is being presented for the partial fulfilment of the degree of **Master in Electrical Engineering** from Jadavpur University, Kolkata-700032.

.....
Prof (Dr.) Debashis Chatterjee
Professor
Department of Electrical
Engineering
Jadavpur University Kolkata,
700032

.....
Prof. Nikhil Mondal
Associate Professor
Department of Electrical Engineering
Jadavpur University
Kolkata, 700032

.....
Prof. Mihir Hembram
Assistant Professor
Department of Electrical Engineering
Jadavpur University
Kolkata, 700032

.....
**Prof. (Dr.) Biswanath
Roy**
Head of the Department of
Electrical Engineering
Jadavpur University
Kolkata, 700032

.....
Prof. (Dr.) Ardhendu Ghoshal
Dean of Faculty Council of
Engineering and Technology
Jadavpur University
Kolkata, 700032

**Faculty of Engineering and Technology
Jadavpur University, Kolkata - 700032**

Certificate of Approval

The forgoing thesis entitled “**Analysis of Stator Active and Reactive Power in a Doubly fed Induction Generator**” is hereby approved as a creditable study of an Engineering subject carried out and presented in a manner that fulfils its acceptance as a prerequisite to the degree for which it is submitted. It is understood that by this approval, the undersigned does not necessarily endorse or approve any statement made, opinion expressed, or conclusion drawn therein but approves the thesis only for the purpose for which it is submitted.

The final examination for evaluation of the thesis

Signature of the examiners

.....

.....

.....

.....

Declaration of Originality

I hereby declare that this thesis contains original research work done by me. All the information in this document has been obtained and presented according to academic rules and ethical conduct. I also declare that, as required by these rules and conduct, I have fully cited and referenced all material and results that are not original to this work.

Name: KUNAL DUTTA

Examination Roll No: **M4ELE23002**
University Registration No: **160164 of 2021-22**

Thesis Title: **Analysis of Stator Active and Reactive Power in a Doubly fed Induction Generator**

Signature with Date:

ACKNOWLEDGEMENTS

I express my sincere gratitude to my supervisor, **Prof. Debashis Chatterjee** for his encouragement, suggestion, and advice, without which it would not have been possible to complete my thesis successfully. I would like to thank **Prof. Nikhil Mondal and Prof Mihir Hembram** for being a constant source of encouragement, inspiration and for their valuable suggestions coupled with their technical expertise throughout my research work. It was a great honour for me to pursue my research under their supervision.

I would also like to thank my co-worker Md. Aadil Hasan, all the staff of the Drives and Simulation laboratory, and the research scholars of our department, specially Mukul Anand, for providing constant encouragement throughout my thesis work.

Finally, I extend my words of gratitude to my parents for personally motivating me to carry out the work smoothly.

ABSTRACT

The thesis studies about the stator active and reactive power variation of a Doubly fed Induction generator (DFIG) at certain rotor speeds by using rotor side converter control technique.

Nowadays, DFIG finds use in a wide range of application, specially in renewable energy sector due to its special case wherein it can operate at a variable speed. The speed of the generator can be above or below the synchronous speed. Hence DFIG can be used at variable slip speeds, and finds extensive use in variable speed wind turbines.

Earlier, wind turbines used to work at a single speed. But the very purpose of wind turbine requires it to work at different speeds according to the speed of the wind at that time. Hence the idea of using DFIG in wind turbines was introduced.

The study of variation of active and reactive power is essential since the wind turbine is used mostly to provide power to the grid, hence enhancing the use of green renewable energy.

CONTENTS

CHAPTER NO.	CONTENTS	PAGE NO.
	Acknowledgement	05
	Abstract	06
	List of Acronyms	09
	List of symbols used	10-11
	List of figures	12-13
	List of tables	14
01	Introduction	15-18
1.1	Motivation for work	16
1.2	Organization of Thesis	17
02	Analysis of Wind Turbine	19-26
2.1	Introduction	19
2.2	Variable speed Wind Turbine	21
2.3	Classification of Wind turbine	24
2.3.1	Variable Speed Wind Turbine	24
2.3.1.1	Type 3 DFIG based Wind Turbine	24
2.3.1.2	Overall structure of Wind Turbine Model	25
03	Analysis of Doubly fed Induction Generator	27-36
3.1	Introduction	27
3.2	Construction of DFIG	27
3.2.1	Working of DFIG	27
3.3	Mathematical Model of DFIG	30
3.3.1	Equivalent Circuit	30
3.3.2	Operating Principle	31
3.3.3	d-q Model in arbitrary reference frame with angular speed	32
	ω_e	
04	Power Flow	37-41
05	Modelling	42-51
5.1	Introduction	42
5.2	Modelling of RSC Converter	42
5.2.1	Value Calculations for Rotor currents	43
5.2.2	DFIG Control Unit	45
5.3	Entire DFIG model	46

5.3.1	Stator Side of the DFIG	47
5.3.2	Rotor Side of the DFIG	49
06	Results and Observations	52-68
6.1	Sub-synchronous Rotor speed=1200 rpm	52
6.1.1-6.1.6	Case study for 6 different reference stator active and reactive power cases	53-63
6.2	Super-synchronous Rotor speed=1700 rpm	64
6.2.1-6.2.	Case study for different reference stator active and reactive power cases	64-67
6.2	Observations	68
7	Conclusion and Future work	70-72
7.1	Conclusion	70
7.2	Scope for future work	70
7.3	References	71

List of Acronyms

SHORT FORM

FULL FORM

FSWT	Fixed Speed Wind Turbine
VSWT	Variable Speed Wind Turbine
AC	Alternating Current
DC	Direct Current
IGBT	Insulated Gate Bipolar Transistor
DFIG	Doubly Fed Induction Generator
PI	Proportional Integration
WT	Wind Turbine
PWM	Pulse Width Modulation
EMF	Electromotive Force
RSC	Rotor Side Controller
PLL	Phase-Locked Loop
PU	Per Unit

List of Symbols

Symbols	Meaning
ρ	Air gap density
R	Blade length of the wind turbine
V	Wind velocity
ω_t	Shaft speed
ω_e	Angular speed of the rotating frame
T_t	Turbine torque
τ_e	Electromagnetic torque
P_t	Turbine Power
β	Pitch angle
I_s, i_r	Stator and rotor current of the DFIG
V_s, V_r, E_r	Stator, rotor and EMF on the rotor side of the DFIG
s	Slip
V_{ds}, V_{qs}	d-q axis voltages of the stator respectively
V_{dr}, V_{qr}	d-q axis voltages of the rotor respectively
i_{ds}, i_{qs}	d-q axis current of the stator respectively
i_{dr}, i_{qr}	d-q axis current of the rotor respectively
$\varphi_{ds}, \varphi_{dr}$	d-axis flux linkage of the stator and rotor respectively(in weber)
$\varphi_{sq}, \varphi_{qr}$	q-axis flux linkage of the stator and rotor respectively(in weber)
φ_m	Mutual flux linkage between the stator and the rotor side

V_{dq_s}, V_{dq_r}	d-q axis voltage of the stator and the rotor side respectively
i_{dq_s}, i_{dq_r}	d-q axis current of the stator and the rotor side respectively
$\varphi_{dq_s}, \varphi_{dq_r}$	d-q axis flux linkage of the stator and the rotor side respectively
R_s, R_r, X_s, X_r	Resistance of the stator and rotor side, reactance of the stator and rotor side
X_m	Mutual reactance between stator and rotor
$P_s, Q_s,$	Active and reactive power on the stator side
P_r, Q_r	Active and reactive power on the rotor side
$P_g,$	Power taken from the grid
P_{rot}	Power fed to the converter
P_{cur}	Rotor copper loss
∂_p, ∂_q	Difference between reference and actual values of active and reactive power

List of Figures

No.	Figure s	Page No.
1.1(a)	Increasing use of Green Energy	16
2.2(a)	Overall working of wind turbine	19
2.1(b)	Internals of Wind Turbine	20
2.2.2(a)	Pitch Angle Controller	22
2.2.6(a)	Wind turbine speed control strategy	23
2.3(a)	Classification of Wind turbine	24
2.3.1.1(a)	DFIG based Wind Turbine	25
2.3.1.2(a)	Overall structure of Wind energy to Electricity conversion	26
3.2(a)	Power Vs RPM curve	28
3.2(b)	Torque Vs RPM curve	29
3.2(c)	Power Vs Wind Speed curve	29
3.3.1(a)	Steady state equivalent circuit of DFIG	30
3.3.2(a)	Equivalent circuit of DFIG in d-axis	33
3.3.2(b)	Equivalent circuit of DFIG in q-axis	33
3.3.2(c)	Overall d-q model of DFIG	33
3.3(a)	Phasor diagram of the rotor side of the DFIG	36
4.1	Power Flow Diagram in DFIG	37
4.2	Bidirectional Converter Block	38
4.3	Sub synchronous and Super synchronous motoring mode	39
4.4	Sub synchronous and Super synchronous generating mode	40
4.5	Detailed representation of power flow in a DFIG	41
5.1(a)	Model for RSC Controller	42
5.2(a)	Model for calculation of rotor currents	43
5.2(b)	Rotor Current Controller	44
5.2.2(a)	Model for Park Transformation	45
5.2.2(b)	Model for Active and Reactive power	46
5.3(a)	Entire Model for the RSC Converter of the DFIG	46
5.3.1(a)	Model for the stator side	47
5.3.1(b)	DFIG Block	48
5.3.1(c)	Model for finding speed and 3 phase stator and rotor currents	48
5.3.1(d)	Angle Calculation Block	49
5.3.2(a)	Model for the rotor side of the DFIG	50
5.3.2(b)	Model for Inverse Park Transform	51
5.3.2(c)	Model for Inverse Clarke Transform	51
6.1	Rotor speed at 1200 rpm	52

6.1.1		
6.1.2	MATLAB graphical results for cases	53-63
6.1.3	6.1.1, 6.1.2, 6.1.3, 6.1.4, 6.1.5, 6.1.6	
6.1.4	(Actual and PU active and reactive power, 3 phase stator voltage and	
6.1.5	stator currents)	
6.1.6		64
6.2	Super-Synchronous rotor speed at 1700 rpm	
	MATLAB graphical results for cases	
6.2.1	6.2.1 and 6.2.2	64-67
6.2.2	(Actual and PU active and reactive power, 3 phase stator voltage and	
	stator currents)	
6.3	Graph for active and reactive power differences	69

List of Tables

SL NO.	TABLE	PAGE NO.
01	Sub-synchronous and super-synchronous motoring mode	39
02	Sub-synchronous and super-synchronous generating mode	40
03	Active and reactive stator power values fed to the DFIG	68
04	Comparison of actual power with the Reference power	68
05	Difference values of active and reactive power with reference	69

CHAPTER 1

INTRODUCTION

With the origin of DFIG in wound rotor induction motors with multiphase winding sets on the rotor and stator, respectively, that was invented by Nikola Tesla in 1888, the rotor winding set of the doubly fed electric machine is connected to a selection of resistors via multiphase slip rings for starting. However, the slip power was lost in the resistors. This means to increase the efficiency in variable speed operation by recovering the slip power were developed. In Krämer (or Kraemer) drive the rotor was connected to an AC and DC machine set that fed a DC machine connected to the shaft of the slip ring machine. Thus the slip power was returned as mechanical power and the drive could be controlled by the excitation currents of the DC machines. The drawback of the Krämer drive is that the machines need to be over dimensioned in order to cope with the extra circulating power. This drawback was corrected in the Scherbius drive where the slip power is fed back to the AC grid by motor generator sets.

The rotating machinery used for the rotor supply was heavy and expensive. Improvement in this respect was the static Scherbius drive where the rotor was connected to a rectifier-inverter set constructed first by mercury arc-based devices and later on with semiconductor diodes and thyristors. In the schemes using a rectifier the power flow was possible only out of the rotor because of the uncontrolled rectifier. Moreover, only sub-synchronous operation as a motor was possible.

Another concept using static frequency converter had a cyclo-converter connected between the rotor and the AC grid. The cyclo-converter can feed power in both directions and thus the machine can be run both sub- and over synchronous speeds. Large cyclo-converter-controlled, doubly fed machines have been used to run single phase generators. Cyclo-converter powered machines can also run the turbines in pumped storage plants.

Today the frequency changer used in applications up to few tens of megawatts consists of two back to back connected IGBT inverters.

Several brushless concepts have also been developed in order to get rid of the slip rings that require maintenance.

The doubly-fed induction generator (*DFIG*) with the back-to-back converter is a system frequently used in wind turbines. Traditional wind turbines have fixed turning speeds, while DFIG enables wind turbines to operate with various range of speeds. The back-to-back converter is connected to the rotor of the DFIG, and its purpose is to feed the rotor with currents of varying frequency, in order to reach the desired rotor speeds. It demonstrates the implementation of a DFIG wind turbine with a back-to-back converter controller. The simulation cases presented in this document cover the stator active and the reactive power response in a DFIG, at two different rotor speeds, one at sub-synchronous speed and the other at super-synchronous speed.

1.1 MOTIVATION FOR WORK

The world, at its present state, is running short on energy. From the advent of industrialization, the requirement of energy has kept on increasing exponentially, and people have been forced to over utilize the non-renewable resources like coal and petroleum. This has not only led to decrease in the levels of non-renewable energy, but also has led to extreme levels of pollution. To curb these issues, harnessing and developing green renewable energy has become the prime objective of all the nations, including India. Increasing demand for electricity, global warming and an excessive amount of carbon emission has led to the development of green and cost-effective energy generation sources around the world. The development of the wind energy green era has also resulted from this.

Over the years, India has seen a huge increase in adoption of green energy, mainly since providing conventional form of energy in a country of almost 1.4 billion is becoming exponentially difficult every day.

The graphical representation shows the increasing use of green energy in India. As can be seen, by 2022, the usage of renewable energy in Gujrat is nearly 18000 MW with nearly equal shares coming from solar and wind sources. Hence it can be inferred that the use of wind as a dominant form of energy is slowing making giant strides in India.

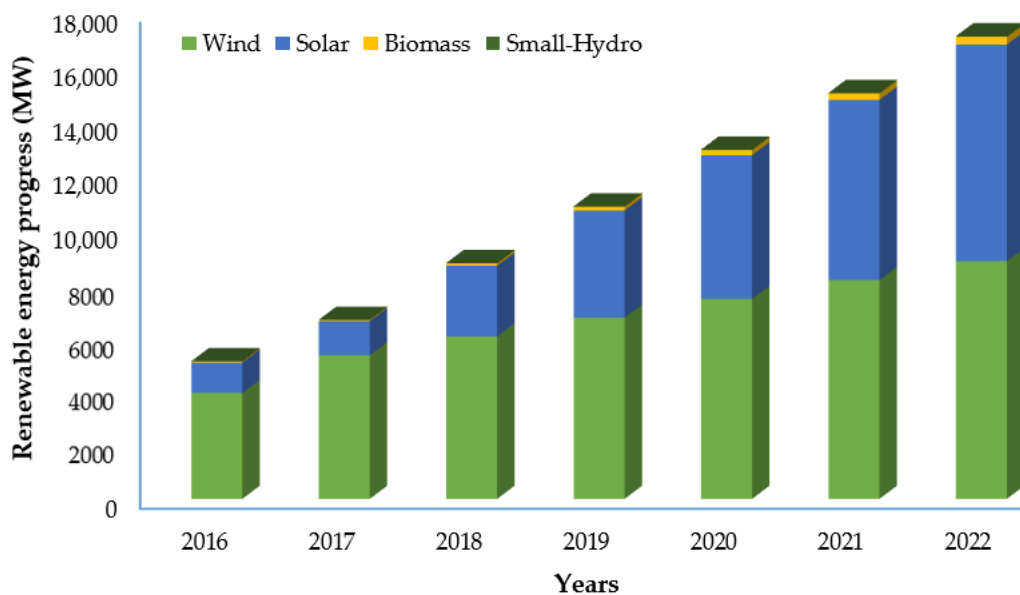


Fig: 1.1 (a): Increasing use of green energy in Gujrat

In Union Budget, 2023, one of the main Saptarishis (7 targets for 2023) was enhancement of renewable energy in India.

As of Feb 2023, Renewable energy sources, including large hydropower, have a combined installed capacity of 178.79 GW.

The following is the installed capacity for Renewables:

- Wind power: 42.6 GW
- Solar Power: 66.7 GW

- Biomass/Co-generation: 10.2 GW
- Small Hydro Power: 4.94 GW
- Waste To Energy: 0.55 GW
- Large Hydro: 46.85 GW

India's target is to produce five million tonnes of green hydrogen by 2030. This will be supported by 125 GW of renewable energy capacity.

From all this data, it can be easily observed that the growth in Wind energy sector is rampant in India, and it provides a big motivation to study the different aspects of wind energy generation.^[19]

Wind energy is developed from the flow of the wind. The harnessing of this energy is comparatively cheaper, and wind being green and renewable source of energy, puts less pressure on the environment and the earth on a whole. This new form of energy is efficient and reduces the use of fossil fuels. It has led to the development of associated technologies for generation of wind energy. One of such technologies or equipment is the Wind Turbine. Wind turbines are generally classified into 2 broad categories: Fixed Speed Wind Turbine (FSWT) and Variable Speed Wind Turbine (VSWT).

1.2 ORGANISATION OF THESIS

The entire thesis is completed in seven (7) chapters.

- **Chapter 1:** outlines the preliminary concept of thesis work. It contains a brief history of Doubly fed induction Generator, my motivation for this work and an outlook about the different chapters and topic of discussion in this thesis.
- **Chapter 2:** Chapter 2 deals with the analysis of a wind turbine, a block diagram including the mechanical and electrical sections and discussion of each block. It also deals with the different types of wind turbines, with special emphasis on the working and structure of type 3 DFIG based wind turbine.
- **Chapter 3:** Chapter 3 deals with the working of DFIG, the various operating curves and principles associated with it. It also discusses the equivalent mathematical circuit, and the nature of power flow.
- **Chapter 4:** This chapter mainly outlines the power flow in a DFIG. This chapter also discusses about the super-synchronous and sub-synchronous nature of motoring and generating action.
- **Chapter 5:** This chapter deals with the entire matlab modelling for stator active and reactive power control using RSC control technique. Here the modelling of the stator side, rotor side of the DFIG is discussed, as well as outlining the rotor current derivation, angle calculation etc.

- **Chapter 6:** This chapter contains the graphical results of various cases for reference active and reactive stator power. The graphs contains initial transient state and final steady state.
- **Chapter 7.** Chapter 7 outlines some conclusion and different avenues for future work.

CHAPTER 2

ANALYSIS OF WIND TURBINE

2.1 INTRODUCTION

A Wind Turbine converts kinetic energy into mechanical energy and this mechanical energy is converted to electrical energy by generator units. The electrical energy is injected into the utility grid with the help of a Power Electronic Converter and step-up transformers and supplied to the user end.

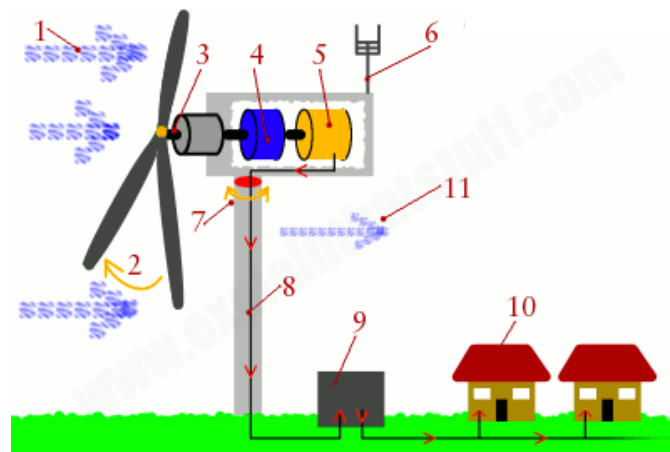


Fig. 2.1(a): Overall working of Wind Turbine ^[16]

1. Wind (moving air that contains kinetic energy) blows toward the turbine's rotor blades.
2. The rotors spin around, capturing some of the kinetic energy from the wind, and turning the central drive shaft that supports them. Although the outer edges of the rotor blades move very fast, the central axle (drive shaft) they're connected to turns quite slowly.
3. In most large modern turbines, the rotor blades can swivel on the hub at the front so they meet the wind at the best angle (or "pitch") for harvesting energy. This is called the pitch control mechanism. On big turbines, small electric motors or hydraulicrams swivel the blades back and forth under precise electronic control. On smaller turbines, the pitch control is often completely mechanical. However, many turbines have fixed rotors and no pitch control at all.
4. Inside the nacelle (the main body of the turbine sitting on top of the tower and behind the blades), the gearbox converts the low-speed rotation of the drive shaft (perhaps, 16 revolutions per minute, rpm) into high-speed (perhaps, 1600 rpm) rotation fast enough to drive the generator efficiently.
5. The generator, immediately behind the gearbox, takes kinetic energy from the spinning drive shaft and turns it into electrical energy. Running at maximum capacity, a typical 2MW turbine generator will produce 2 million watts of power at about 700 volts. 19

6. Anemometers (automatic speed measuring devices) and wind vanes on the back of the nacelle provide measurements of the wind speed and direction.
7. Using these measurements, the entire top part of the turbine (the rotors and nacelle) can be rotated by a yaw motor, mounted between the nacelle and the tower, so it faces directly into the oncoming wind and captures the maximum amount of energy. If it's too windy or turbulent, brakes are applied to stop the rotors from turning (for safety reasons). The brakes are also applied during routine maintenance.
8. The electric current produced by the generator flows through a cable running down through the inside of the turbine tower.
9. A step-up transformer converts the electricity to about 50 times higher voltage so it can be transmitted efficiently to the power grid (or to nearby buildings or communities). If the electricity is flowing to the grid, it's converted to an even higher voltage (130,000 volts or more) by a substation nearby, which services many turbines.
10. Homes enjoy clean, green energy: the turbine has produced no greenhouse gas emissions or pollution as it operates.
11. Wind carries on blowing past the turbine, but with less speed and energy (for reasons explained below) and more turbulence (since the turbine has disrupted its flow).^[18]

Inside of a wind turbine is shown below.

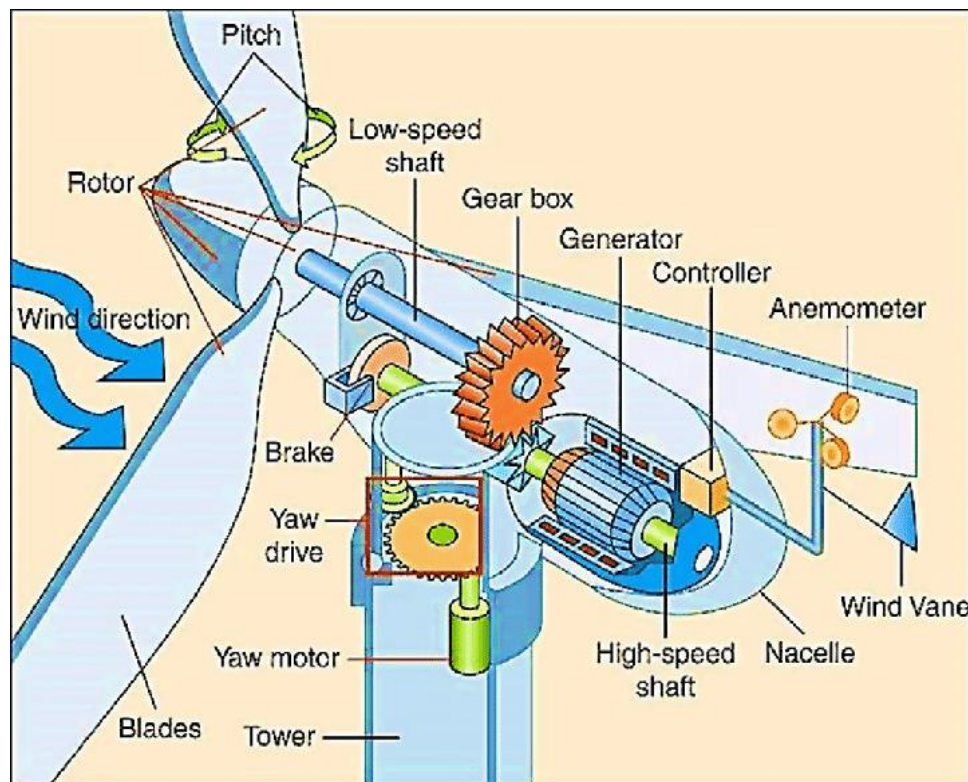


Fig. 2.1(b): Internals of a Wind Turbine^[16]

2.2 VARIABLE SPEED WIND TURBINE

The model of a variable speed wind turbine is shown in the figure below.

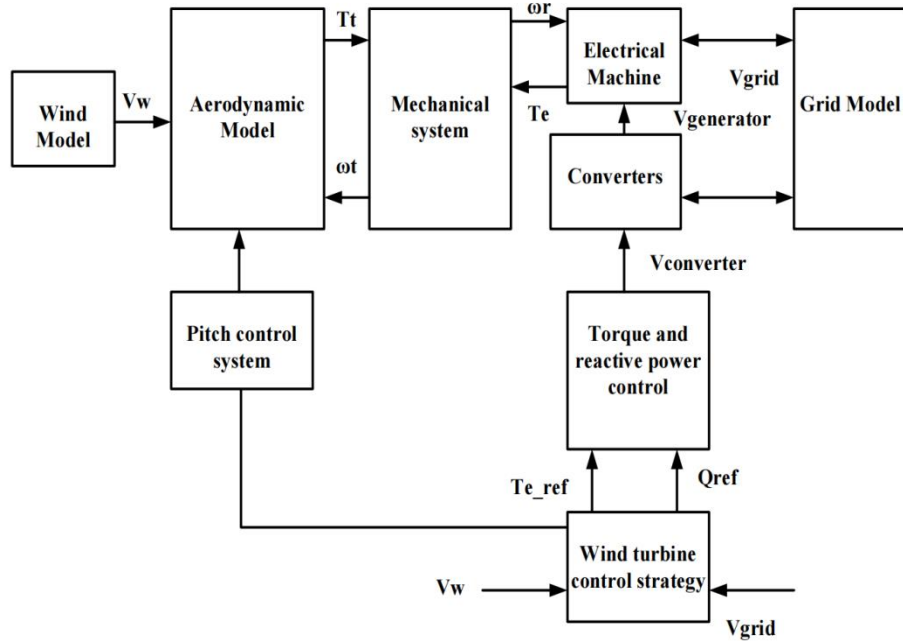


Fig. 2.2(a): Variable speed wind turbine

The different components of this model are as follows:

- Aerodynamic Model^[06]

It measures the power extraction of the machine rotor. The wind aerodynamics model evaluates the turbine power (P_t) which is dependent on power coefficient (C_p). The power generated by the rotor is expressed as

$$P_t = \left(\frac{1}{2}\right)C_p\rho R^2V^3 \quad (2.1)$$

where ρ is the air density, R is the blade length and V is the wind velocity.

The shaft speed being ω_t , the turbine torque will be expressed as

$$T_t = \left(\frac{P_t}{\omega_t}\right) \quad (2.2)$$

C_p is the power angle coefficient and it depends upon the tip-speed ratio (λ) and the pitch angle (β). The tip-speed ratio or TSR, denoted by λ , is the ratio of the blade-tip linear speed to the wind speed. K_1 to K_8 are the constants where,

$$C_p = K_1 \left(\frac{K_2}{\lambda_1} - K_3 \beta - K_4 \beta^{K_5} - K_6 \right) \left(e^{\frac{K_7}{\lambda_i}} \right) \quad (2.3)$$

$$\lambda_i = \frac{1}{\lambda + 8} \quad (2.4)$$

- Pitch Angle Controller

The pitch angle controller is designed for the WT's blades to rotate at the same angle. The pitch angle controller is there to provide independent rotation of the blades at the same angle. The pitch angle (β) of the blades of the wind turbine is controlled by this controller. The controller helps to limit the wind power captured at the rated turbine power.

Figure below shows the block diagram of the blade pitch angle controller.

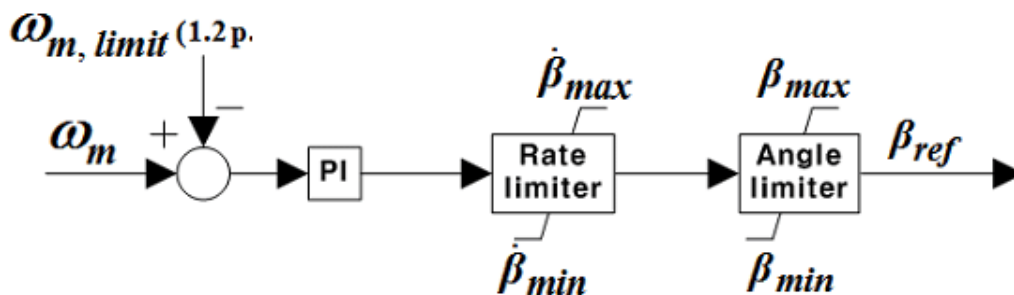


Fig. 2.2.2(a) Pitch Angle Controller ^[16]

- Mechanical system consists of the blades coupled with a shaft system that is further linked to the gearbox. This mechanical system of a WT evaluates the angular speed of the generator and turbine. It forms a link between mechanical and electrical systems. This mechanical system of a WT evaluates the angular speed of the generator and turbine, in terms of turbine torque and generator torque .

- Electrical Energy and Converter

Electrical machines are mainly run by power electronic converters. Mainly Doubly Fed Induction Generators and Permanent Magnet Synchronous Generators are used in modern day variable speed wind turbine.

- Control Unit

A control unit checks the pitch angle, generator torque, active and reactive power and controls the converters accordingly.

- Speed Controller

This controller maintains the generator speed at a specific value for tracking the maximum power. It also generates the reference active power (P_{ref}) for the generator.

The wind turbine speed control strategy is illustrated in Fig.2.2.6 (a). It is classified into four zones. Zone 1 limits the minimum speed of operation. The generator starts to run at cut in wind speed with a rotating speed Ωm_{min} .

Zone 2 is used to follow the maximum power extraction at variable speed with respect to a load. With the increase in wind speed, the speed of rotation also gets enhanced until the maximum speed of rotation Ωm_{max} is reached.

Generator now operates in Zone 3 and limits the maximum speed at parallel operation. The energy captured at higher wind speed is regulated at this nominal value.

The energy captured in Zone 4 corresponds to the full load operation and limits the maximum operating speed at rated power output.

The mechanical power is controlled by varying the pitch angle control or by torque control. The electromagnetic torque (T_e) is controlled at nominal speed through torque control and the pitch angle is adjusted to keep the turbine at maximum speed and rated power.

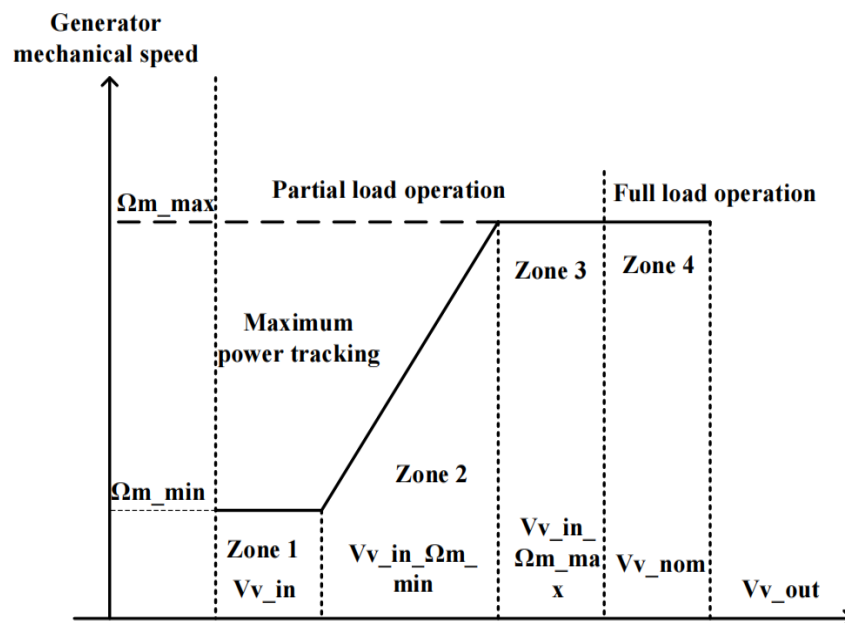


Fig. 2.2.6(a): Wind turbine speed control strategy

2.3 CLASSIFICATION OF WIND TURBINES

Wind turbines are classified into 2 broad categories as discussed in the figure below.

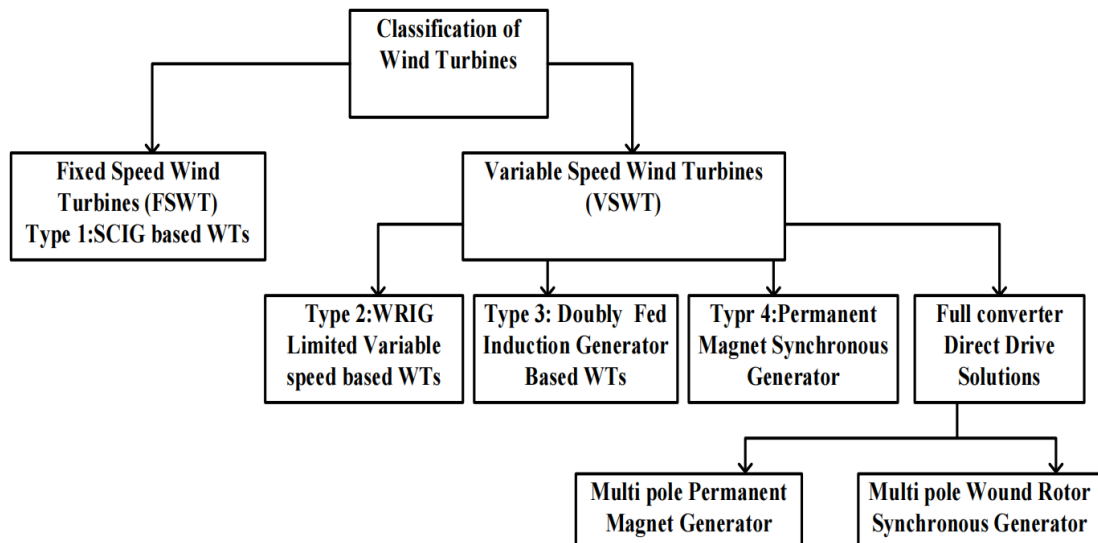


Fig. 2.3(a): Classification of Wind turbine

Here we are going to discuss about Variable speed wind turbine, mainly type 3, which is DFIG based wind turbines.

2.3.1 Variable Speed Wind Turbine

Variable speed wind turbines are much advanced than fixed speed ones since it is more practical and have many real-life applications. Power control is provided by pitch able blades. Here power electronic converter allows higher and maximum energy at variable speeds.

2.3.1.1 Type 3 DFIG based Wind Turbine

A variable speed wind turbine with Doubly-Fed Induction Generator (DFIG) is known as Type 3 Wind Turbine. The schematic of Type 3 WT is shown in Figure below.

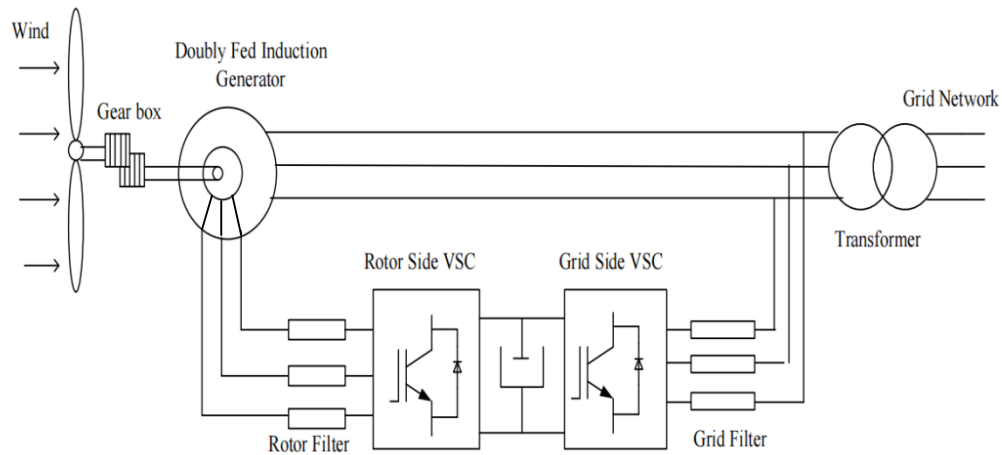


Fig. 2.3.1.1 (a): DFIG based Wind Turbine

The use of DFIG based wind turbines has proved to be very successful in power generation. DFIG is a traditional Wound Rotor Induction Generator along with power electronic converters which are externally connected to the stator and rotor.

As shown in Figure 2.3.1.1(a), the stator circuit is directly connected to the grid. The rotor side and grid side converters respectively rectify the grid voltage and convert it into AC voltage which is given as an excitation to the rotor.

2.3.1.2 OVERALL STRUCTURE OF WIND TURBINE MODEL

The grid connected wind turbine considered here applies a DFIG, using back to back PWM voltage source converters in the rotor circuit. The complete grid connected wind turbine model includes the wind speed model, the aerodynamic model of the wind turbine, PWM voltage source converters, and the control system. Fig. 2.3.1.2(a) shows the overall structure of the grid connected wind turbine model.

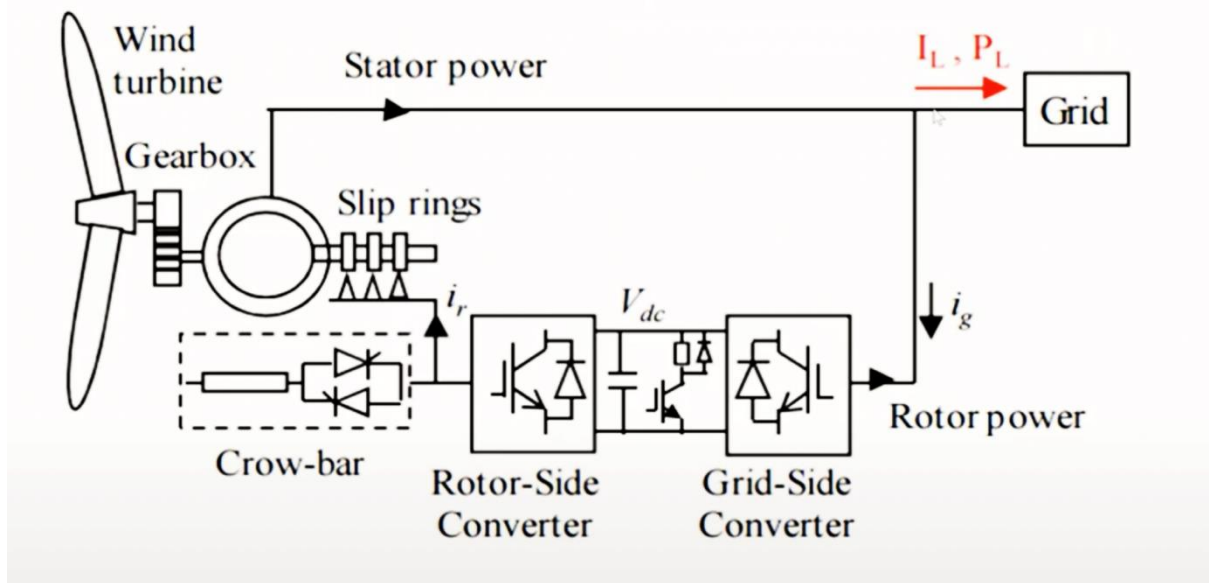


Fig. 2.3.1.2(a): Overall structure of Wind energy to Electricity conversion

As the wind turbines rotate, they exert mechanical force on the rotor, causing it to rotate. As the rotor rotates the magnetic field produced due to the ac current also rotates at a speed proportional to the frequency of the ac signal applied to the rotor windings. As a result a constantly rotating magnetic flux passes through the stator windings which cause induction of ac current in the stator winding. Thus the speed of rotation of the stator magnetic field depends on the rotor speed as well as the frequency of the ac current fed to the rotor windings

The basic requirement for the electricity generation using wind energy is to produce ac signal of constant frequency irrespective of the wind speed. In other words the frequency of the ac signal generated across the stator should be constant irrespective of the rotor speed variations. To achieve this, the frequency of ac signal applied to the rotor windings need to be adjusted.

The whole system consists of two back to back converters – a machine side converter and a grid side converter, connected in the feedback loop of the system. The machine side converter is used to control the active and reactive powers by controlling the d-q components of the rotor and also torque and speed of the machine. The grid side converter is used to maintain a constant dc link voltage and ensures the unity power factor operation by making the reactive power drawn from the utility grid to zero.

A capacitor is connected between the two converters such that it acts as an energy storage unit. This back to back arrangement provides a fixed voltage fixed frequency output irrespective of the variable frequency, variable voltage output of the generator. Other applications of the induction generators are fly-wheel energy storage systems, pumped storage power plants, power converters feeding a railway power grid from public grid where the frequency is fixed.

CHAPTER 3

ANALYSIS OF DOUBLY FED INDUCTION GENERATOR

3.1 INTRODUCTION

A Doubly Fed Induction generator as its name suggests is a 3 phase induction generator where both the rotor and stator windings are fed with 3 phase AC signal. It consists of multi-phase windings placed on both the rotor and stator bodies. It also consists of a multi-phase slip ring assembly to transfer power to the rotor. It is typically used to generate electricity in wind turbine generators.

Induction machines are usually singly fed but they can be easily doubly fed if we can somehow make the rotor terminals accessible. And the rotor terminals can be made accessible only in case of a wound rotor induction machine. In a wound rotor machine the system can be controlled through the rotor.

3.2 CONSTRUCTION OF DFIG

In case of a wound rotor induction machine the stator and rotor constructions are identical, for example a stator winding for N poles will have a rotor winding for N poles as well.

For a 3 phase induction machine the rotor must have 6 terminals that is 2 terminals for each phase, and then the terminals are electrically shorted and connected to slip rings. (the terminals must be internally connected in such a way so that the star or delta connection can be achieved and then the terminals are connected to the 3 slip rings which are further externally connected with brushes)

The main disadvantage with such wound rotor machine is that the complicated structure of slip rings and brushes must be brought out to the terminals

3.2.1 WORKING OF DFIG

Now we can apply a voltage to the rotor. We must apply supply with a frequency equal to the slip frequency of the induction machine. Hence in case of a doubly-fed machine we can provide power to the motor both from the stator side as well as from the rotor side

Example: P_1 power input through the stator P_2 power input through the rotor will result in $(P_1 + P_2)$ power output through the shaft.

similarly P_1 power input to the stator and P_2 power output through the rotor will result in $(P_1 - P_2)$ power output through the shaft.

Hence P_1 and P_2 can be both positive and negative depending upon the direction of power flow, so this doubly fed machine can work as a motor, as a generator, as a sub synchronous machine, as a super synchronous machine

Now we shall discuss the power versus rotational speed characteristics of a power turbine for different wind speeds. Here it must be noted that the rotational speed of the turbine and the wind speed has no direct relationship. the figure below shows the characteristics.

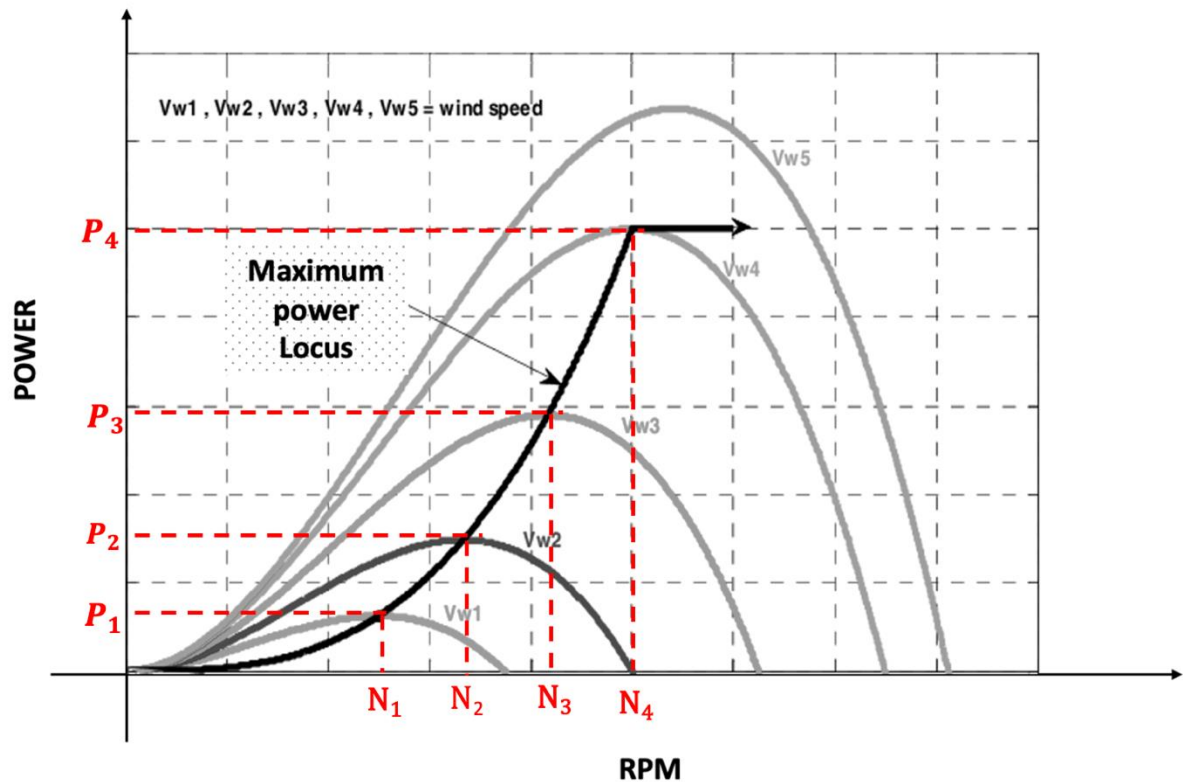


Fig. 3.2(a): Power VS RPM curve

Our objective is to obtain maximum power for any possible wind speed, accordingly we can form the locus of the maximum power as shown in the figure.

The different maximum power for the different wind speed ($V_{w1} < V_{w2} < V_{w3} < V_{w4}$) along the maximum power locus are represented by P_1, P_2, P_3, P_4 and the corresponding rpm of the wind turbine are represented by N_1, N_2, N_3, N_4 respectively.

Similarly the power speed characteristics of an induction generator is shown in figure 3.2(a)

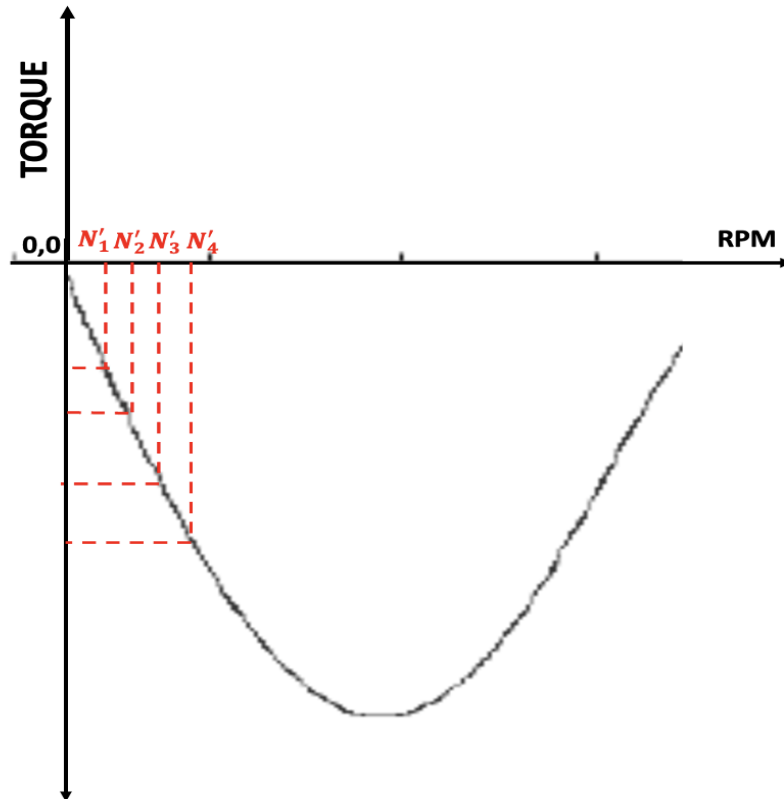


Fig. 3.2(b): Torque vs RPM curve

In the figure 3.2(b) we plot the different maximum power points (P_1 P_2 P_3 P_4) and accordingly get the speed of the induction generator (N'_1 N'_2 N'_3 N'_4). Our objective is to match the characteristics of the wind turbine with the characteristics of the generator.

Here figure 3.2(c) shows the power versus wind speed characteristics. We don't prefer to operate the turbine at a very low wind speed (Region 1). The cut-in speed is the wind speed above which the turbine operates. We also have a parameter called cut-out speed, when the wind speed is above cut-out speed the turbine does not work since the phenomenon called Gusting may damage the blades of the turbine. So we prefer to operate the wind turbine at a wind speed in region 2 and 3

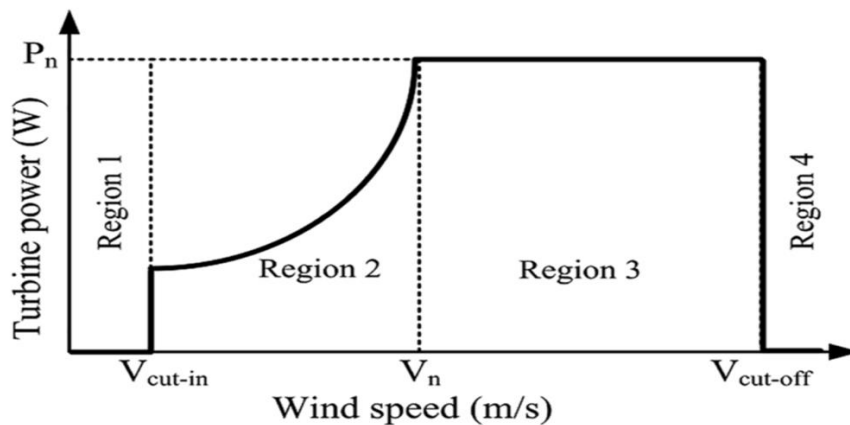


Fig. 3.2(c): Power Vs Wind Speed curve

3.3 MATHEMATICAL MODEL OF DFIG

3.3.1 EQUIVALENT CIRCUIT

The figure 3.3.1(a) shows the rotor quantities brought in terms of the stator values that is the stator equivalent of the circuit.

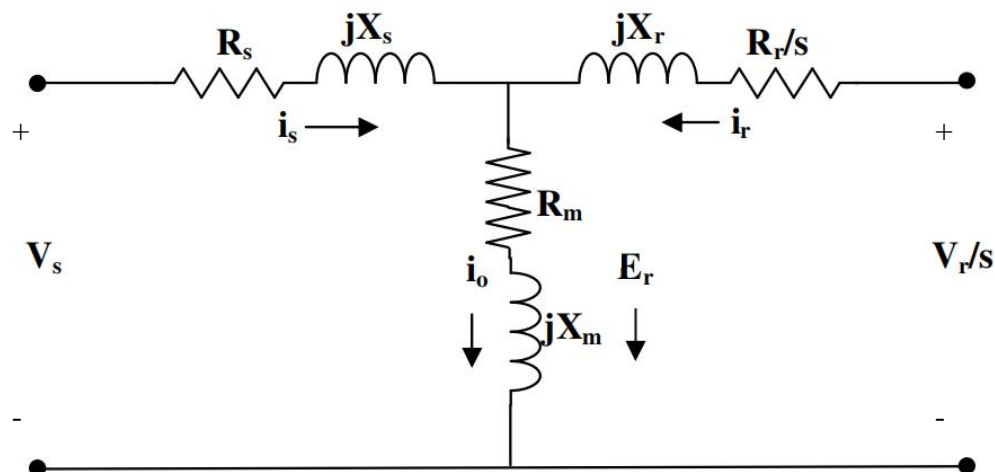


Fig. 3.3.1(a): Equivalent circuit of DFIG

The modelling of DFIG is based on generalised theory of machines. First we analyse the steady state equivalent circuit of DFIG. Fig 3.3.1(a) shows the diagram of the steady state equivalent circuit of the DFIG, where the quantities on the rotor side are referred to the stator side.

This equivalent circuit is basically similar to an induction machine when the parameters are referred to the stator side.

The direction of i_r may be feeding into V_r/s or going out from V_r/s , this power flow is controllable

In fig 3.3.1(a)

- V_s and V_r represents the applied stator and rotor phase voltage to the induction machine respectively

- E_r is the EMF
- I_s is the stator current
- I_r is the rotor current
- I_0 is the no load current
- R_s is the stator resistance
- R_r is the rotor resistance
- X_s and X_r represents the stator and the rotor leakage reactance
- R_m represents the magnetizing losses
- X_m is the magnetizing reactance
- s is the generator slip.

The circuit parameters are stator equivalent. All the parameters are brought to the stator. Applying Kirchhoff's voltage law to the circuit in Fig. 3.3.1 (a) we get,

$$\text{Stator side equation: } V_s = (R_s + jX_s) * i_s - E_r \quad (3.1)$$

$$\text{Rotor side Equations: } \frac{V_r}{s} - i_r * (R_r/s + jX_r) - E_r = 0$$

$$V_r - i_r * (R_r + jsX_r) = sE_r \quad (3.2)$$

$$E_r = -(R_m + jX_m) * i_0 \quad (3.3)$$

$$i_0 = i_s + i_r \quad (3.4)$$

Equation 3.2 will be later used to draw the phasor diagram.

3.3.2. OPERATING PRINCIPLE

For a normal wound rotor induction generator with short circuited rotor, i.e. the applied voltage to the rotor V_r is zero, the relationship between the Torque T_e and the current in the rotor can be stated as

$$T_e = K\phi_m i_r \quad (3.5)$$

Where K is the constant, ϕ_m is the air gap magnetic flux per phase in wb, and i_r is the rotor current.

The real current in the rotor is expressed as in equation 3.6

$$\begin{aligned} I_r &= \frac{sE_r}{\sqrt{(R_r^2 + (sX_r)^2)}} * \frac{R_r}{\sqrt{(R_r^2 + (sX_r)^2)}} \\ &= \frac{sE_r R_r}{\sqrt{(R_r^2 + (sX_r)^2)}} \end{aligned} \quad (3.6)$$

Rotor reactance is very small in comparison to the rotor resistance, hence we can approximate the rotor current equation to

$$I_r = \frac{sE_r R_r}{\sqrt{(R_r^2 + (sX_r)^2)} \sim \frac{sE_r}{R_r} \quad (3.7)$$

The voltage applied to the induction generator, being assumed constant, the rotor current i_r can also be assumed constant.

When an external voltage is applied to the rotor circuit,

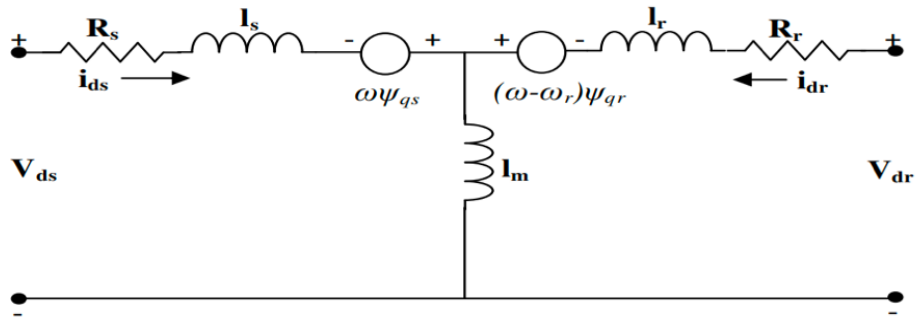
$$I_r = \frac{sE_r + V_r}{R_r} \quad (3.8)$$

Therefore, it is possible to control the speed of the generator as well as the stator side power factor by modulating the magnitude and phase of the applied voltage, while keeping the electromagnetic torque constant.

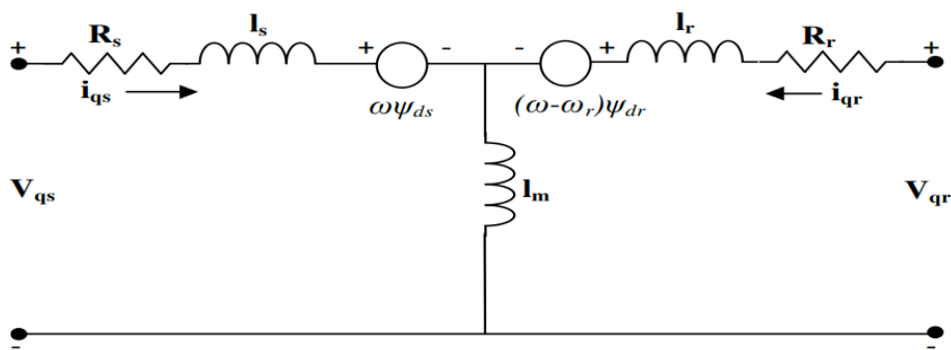
3.3.3. d-q MODEL IN THE ARBITRARY REFERENCE FRAME WITH AN ANGULAR SPEED ω_e

The stator and the rotor windings are transformed to their two-phase equivalent using the park or dq0- transformation based on complex equivalent circuit of DFIG as shown in Fig 3.3.2(c). By using the d - q model, three to two phase representations are described.

Fig 3.3.2 (a, b) shows the equivalent circuit of DFIG in d and q axis respectively



(a)



(b)

Fig. 3.3.2: Equivalent circuit of DFIG in d-q axis respectively

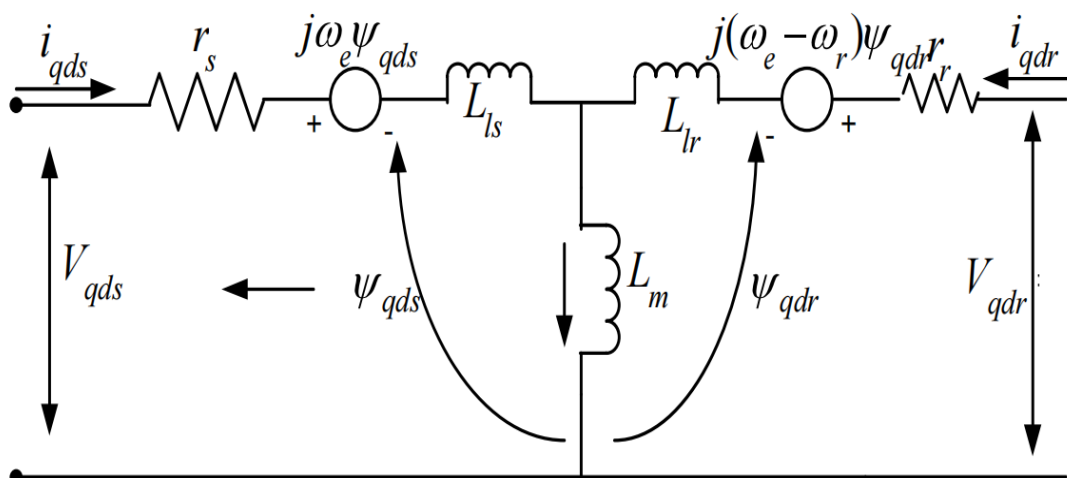


Fig. 3.3.2 (c): overall d-q circuit

The following assumptions are made for developing the d - q model of induction machine [31]:

- Iron losses are neglected.
- Stator and rotor skin effects are neglected.
- Magnetizing inductance saturation is neglected.
- Constant air gap reluctance.
- Stator and rotor windings of the DFIG are assumed symmetric.
- Windings are assumed as sinusoidally distributed.

The transformation matrix is expressed in the eqn. (3.9)

$$[P] = \begin{bmatrix} \cos \theta & \cos(\theta - 120^\circ) & \cos(\theta + 120^\circ) \\ -\sin \theta & -\sin(\theta - 120^\circ) & -\sin(\theta + 120^\circ) \end{bmatrix} \quad (3.9)$$

Where θ is the angle between the a - b - c and d - q axis.

The mathematical model according to Park's transformation for the stator and rotor voltage in an arbitrary d-q axis rotating frame with an angular speed ω_e is discussed below

$$V_{ds} = i_{ds}R_s + \frac{d\phi_{ds}}{dx} - \omega_e\phi_{qs} \quad (3.10)$$

$$V_{qs} = i_{qs}R_s + \frac{d\phi_{qs}}{dx} + \omega_e\phi_{ds} \quad (3.11)$$

$$V_{dr} = i_{dr}R_r + \frac{d\phi_{dr}}{dx} - \omega_e\phi_{qr} \quad (3.12)$$

$$V_{qr} = i_{qr}R_r + \frac{d\phi_{qr}}{dx} + \omega_e\phi_{dr} \quad (3.13)$$

Stator and rotor fluxes are magnetically decoupled in d and q axis respectively as follows

$$\phi_{ds} = L_s i_{ds} + L_m i_{dr} \quad (3.14)$$

$$\phi_{qs} = L_s i_{qs} + L_m i_{qr} \quad (3.15)$$

$$\phi_{dr} = L_r i_{dr} + L_m i_{ds} \quad (3.16)$$

$$\phi_{qr} = L_r i_{qr} + L_m i_{qs} \quad (3.17)$$

A synchronous reference frame based circuit of DFIG is shown in figure 3.3.2(c)

Using equations 3.10 to 3.13, combining d-q axis together to find stator and rotor voltages, we get

$$V_{dqs} = i_{dqs} * R_s + \frac{d\varphi_{dqs}}{dx} + j\omega_e \varphi_{dqs} \quad (3.18)$$

$$V_{dqr} = i_{dqr} * R_r + \frac{d\varphi_{dqr}}{dx} + j\omega_e \varphi_{dqr} \quad (3.19)$$

$$\varphi_{qds} = L_s i_{dqs} + L_m i_{dqr} \quad (3.20)$$

$$\varphi_{qdr} = L_s i_{dqr} + L_m i_{dqs} \quad (3.21)$$

Where i_{qds} and i_{qdr} are the complex conjugates of the stator and rotor current vector. The stator and rotor inductances are given by

$$L_s = L_{ls} + L_m \quad (3.22)$$

$$L_r = L_{lr} + L_m \quad (3.23)$$

Where L_m is the mutual inductance consequently, Active and Reactive powers on stator and rotor side are defined as^[06]

$$P_s = V_{ds} i_{ds} + V_{qs} i_{qs} \quad (3.24)$$

$$Q_s = V_{qs} i_{qs} - V_{ds} i_{ds} \quad (3.25)$$

$$P_r = V_{dr} i_{dr} + V_{qr} i_{qr} \quad (3.26)$$

$$Q_r = V_{qr} i_{qr} - V_{dr} i_{dr} \quad (3.27)$$

In the above equations

$V_{ds}, V_{dr}, V_{qs}, V_{qr}, i_{ds}, i_{qs}, i_{dr}, i_{qr}$ are the stator and rotor voltages and current in d-q axis reference frame. Suffix d, q denotes axis and suffix s, r denotes stator and rotor values respectively.

$\varphi_{ds}, \varphi_{qs}, \varphi_{dr}, \varphi_{qr}$ represent the stator and rotor fluxes in d-q axis reference frame.

R_s and R_r are the stator and rotor winding resistances

L_s, L_r, L_m are the stator, rotor and mutual inductances

ω_s is the reference speed which depends upon the supply frequency and the no of poles of the machines, and ω_r is the rotor rotational speed.

P_s, Q_s, P_r, Q_r are active and reactive power of stator and rotor side of DFIG system

We can draw the phasor diagram by applying KVL in the rotor side from fig 3.3.1(a), using equation 3.2

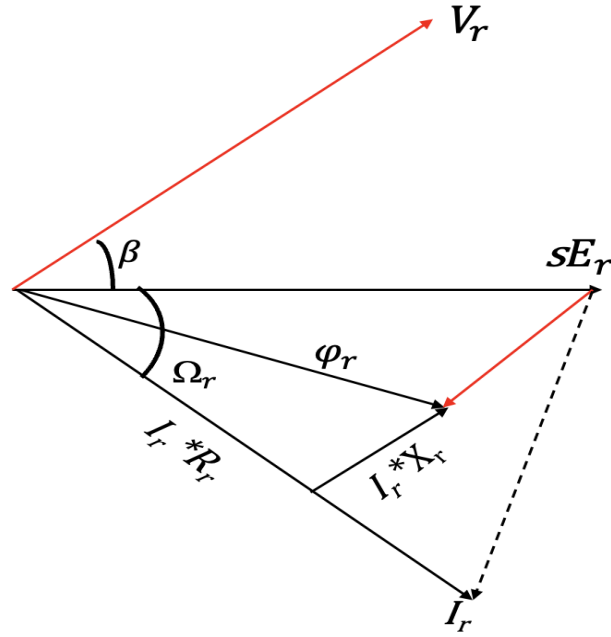


Fig. 3.3(a): Phasor diagram of the rotor side of the DFIG

(The direction of i_r is considered feeding into V_r/s)

$$sV_g - I_r * (R_r + jsX_{lr}) - E_g = 0 \quad (3.28)$$

$$(sV_g - E_g) = I_r * (R_r + jsX_{lr})$$

From the phasor diagram, solving all components along i_r axis

$$sE_r * \cos(\Omega_r) = I_r * R_r + V_r \cos(\Omega_r + \beta)$$

$$sE_r * I_r * \cos(\Omega_r) = I_r^2 * R_r + V_r I_r \cos(\Omega_r + \beta) \quad (3.29)$$

On a three phase basis: $3 * E_r * I_r * \cos(\Omega_r) = P_g =$ power taken from the grid

$$3 * I_r^2 * R_r = P_{cur} = \text{Rotor copper loss}$$

$$3 * V_r * I_r * \cos(\Omega_r + \beta) = P_r = \text{Power fed to the converter}$$

$$\text{Hence: } sP_g = P_{cur} + P_r \quad (3.30)$$

This is shown in the figure below (Figure of power flow fig 4.1). This is shown for power flowing into V_r , similarly another phasor can be drawn for power flowing out of V_r

CHAPTER 4

POWER FLOW

The schematic diagram of a doubly-fed induction machine and the power flow is shown below

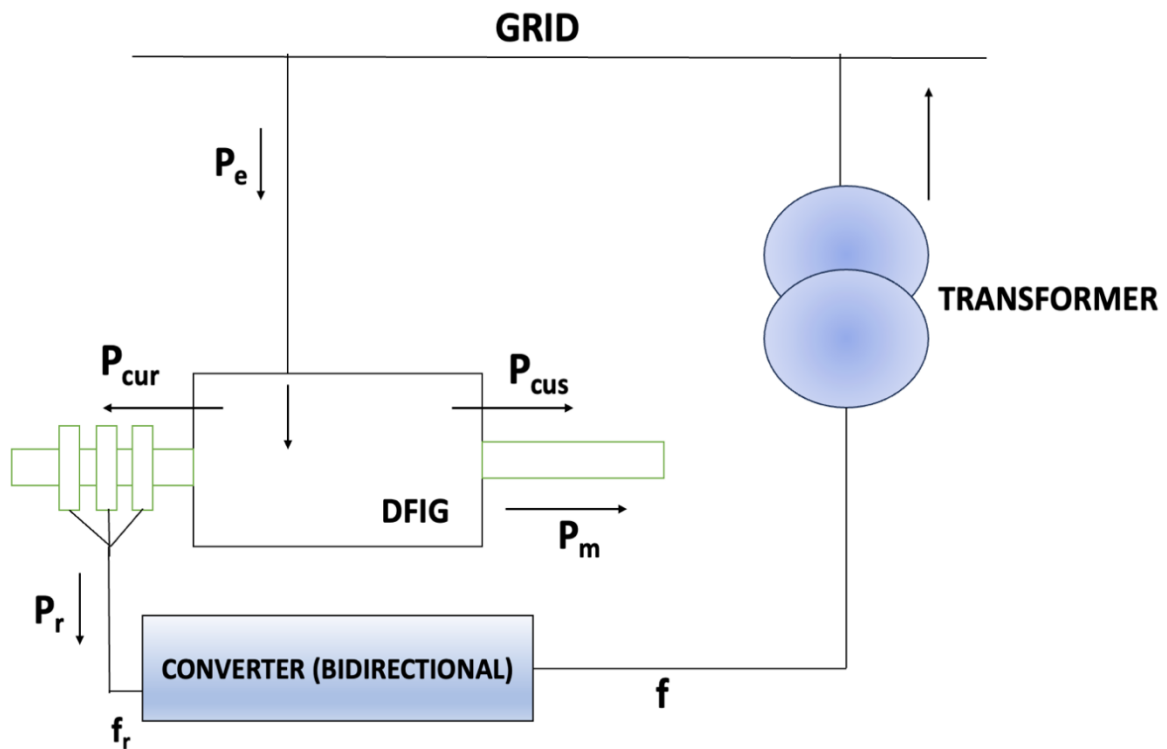


Fig. 4.1: Power Flow Diagram in DFIG

$P_e = P_g$ is the power drawn from the grid into the doubly-fed induction generator. This power is also called the air gap power. From P_g , stator copper loss (P_{cus}), rotor copper loss (P_{cur}), rotor power (P_r) and the shaft power (P_m) are drawn.

Rotor power (P_r) = 0, in traditional induction generator or motor since no external power is supplied to the rotor body.

Excluding stator copper loss (P_{cus}) and rotor copper loss (P_{cur}),

Rotor power (P_r) = $s * P_g$

Mechanical power given to the load $P_m = (1 - s) * P_g$ where s = slip of the generator.

The converter block shown in the block diagram is as follows. The importance of the converters are discussed later.

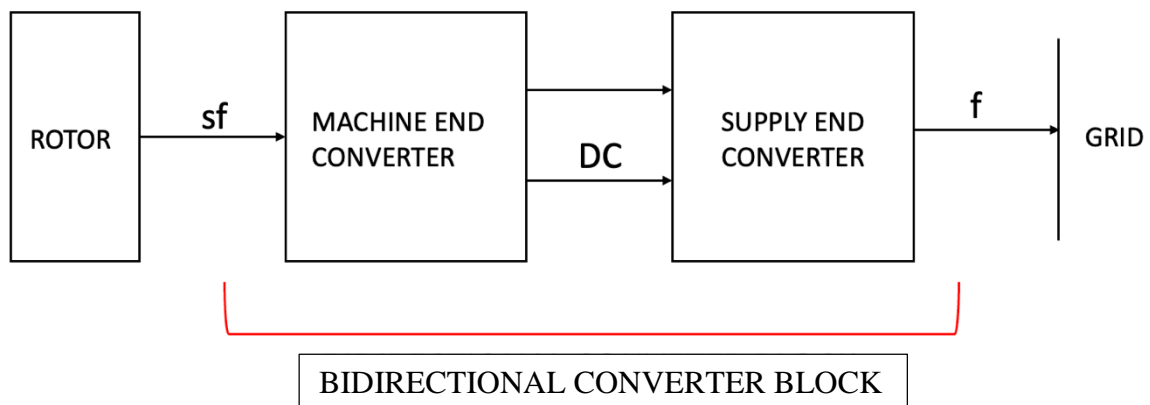


Fig. 4.2: Bidirectional Converter Block

NOTE THAT HERE THE SLIP CAN HAVE NEGATIVE VALUES AS WELL.
Accordingly 4 cases may arise

Case 1: Sub-synchronous motoring

- $0 < s < 1$; slip is positive
- P_g, P_r, P_m are positive

Case 2: Super-synchronous Motoring

- $-1 < s < 0$; slip is negative
- P_g, P_m are positive
- P_r is negative
- $(P_m) = (1-s)*P_g$ is positive, that is P_m is more than P_g

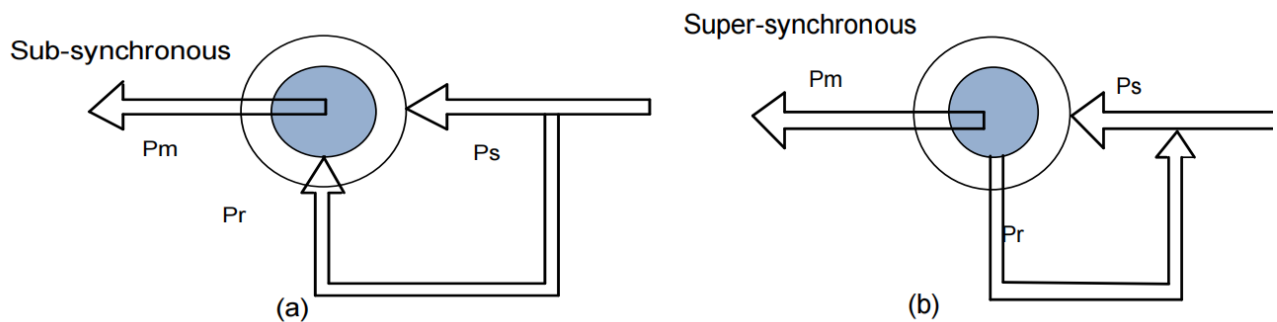


Fig. 4.3: Sub synchronous and super synchronous motoring mode

Speed	Mechanical Power(P_m)	Stator Active Power(P_s)	Rotor Active Power(P_r)
Sub synchronous $s > 0$ and $\omega_m < \omega_s$	$P_m > 0$	$P_s > 0$	$P_r > 0$
Super synchronous $s < 0$ and $\omega_m > \omega_s$	$P_m > 0$	$P_s > 0$	$P_r < 0$

Hence a doubly fed machine can perform motoring action even beyond the rated speed.

Case 3: Sub-synchronous Generating

- $0 < s < 1$; slip is positive
- P_g, P_r, P_m are negative
- $(P_m) = (1-s)*P_g$ is negative, that is P_m is less than P_g

Case 4: Super-synchronous Generating

- $-1 < s < 0$; slip is negative
- P_g, P_m are negative
- P_r is positive
- $(P_m) = (1-s)*P_g$ is negative, that is P_m is more than P_g

Speed	Mechanical Power (P_m)	Stator Active Power (P_s)	Rotor Active Power (P_r)
Sub synchronous $s > 0$ and $\omega_m < \omega_s$	$P_m < 0$	$P_s < 0$	$P_r > 0$
Super synchronous $s < 0$ and $\omega_m > \omega_s$	$P_m < 0$	$P_s < 0$	$P_r < 0$

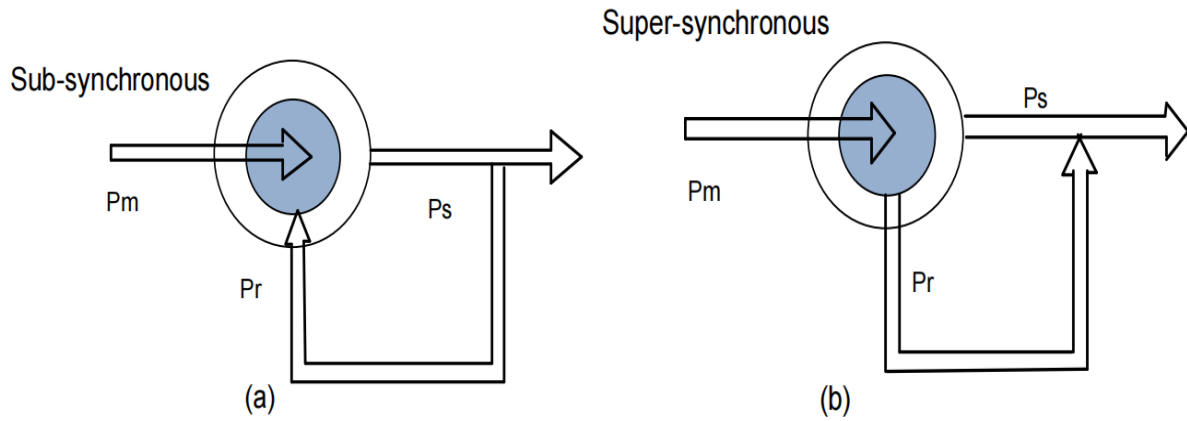


Fig. 4.4: Sub synchronous and Super synchronous generating mode

Super synchronous generator case is used in case of a wind turbine, because we get more power at the shaft than the air gap power.

Now look into the case in a bit more detail by taking an example

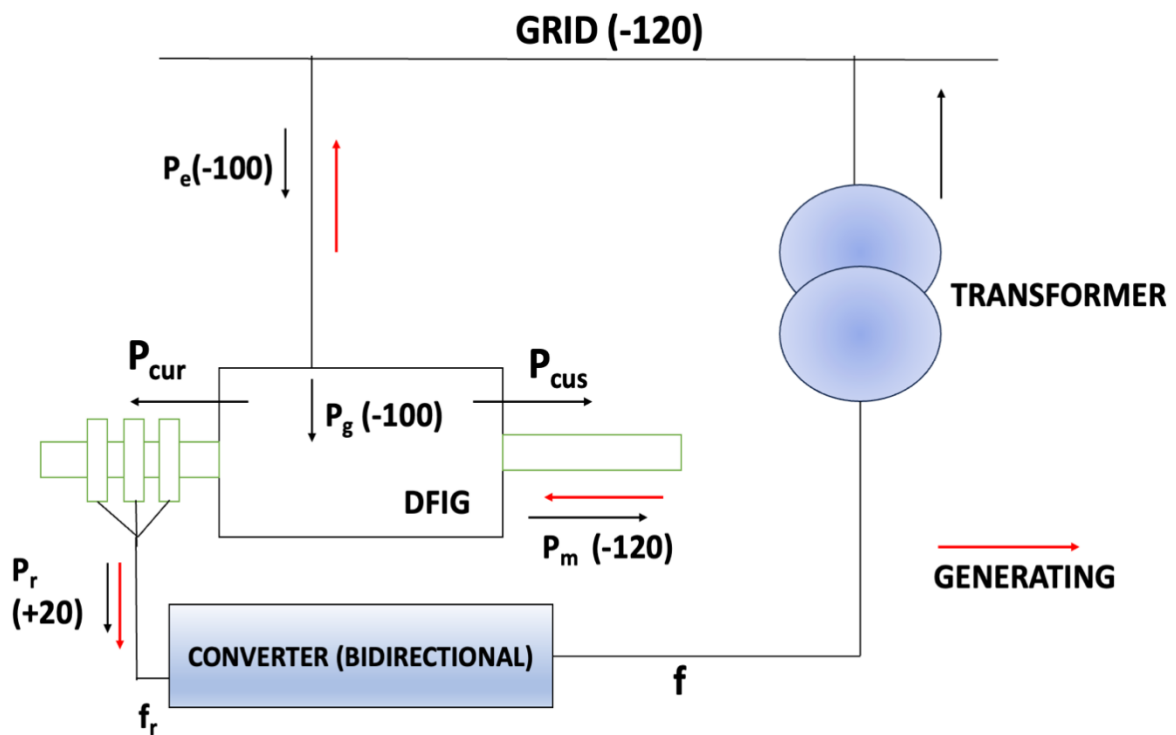


Fig. 4.5: Detailed representation of power flow in a DFIG

For slip $s = -0.2$

$P_g = -100$ units that is 100 units of power is fed to the grid

$$(P_m) = (1-s)*P_g = -120 \text{ units}$$

$$(P_r) = s* P_g = 20 \text{ units}$$

Here, P_m is delivering 120 units of power into the doubly-fed machine hence working as a generator.

- From the 120 units of power 100 units of power are fed to the grid and 20 units of power are drawn by the rotor. The 20 units of power goes to the converter and again feeds the grid therefore the total power fed to the grid becomes 120 units of power. Here P_g is negative, P_m is negative but P_r is positive.

Here we observe that the air gap power is only 100 units while the shaft power is 120 units.

CHAPTER 5

MODELLING

5.1 INTRODUCTION

We are interested in controlling the active and reactive power flow in a DFIG with variable speed wind turbine. We are going to introduce the rotor side control method.

A vector control technique is applied to the rotor side converter so that we can control the stator side active and reactive power. The direct axis loop is used to control reactive power whereas the quadrature axis is for active power control. A stator flux oriented vector control is applied to the rotor side converter. Fig 5.1(a) shows the MATLAB model of the RSC controller

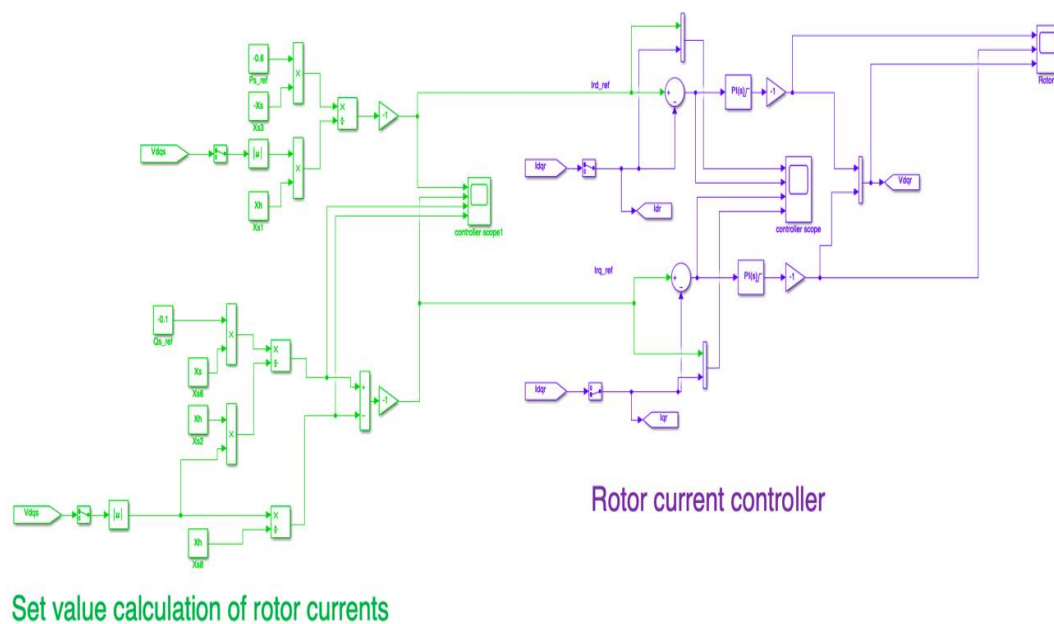


Fig 5.1(a): Model of RSC Controller

5.2 MODELLING OF RSC CONTROLLER

Figure 5.1 is the entire MATLAB model for RSC Controller. For further explanation we divide the figure into 2 parts:

Fig 5.2(a): Value calculation for rotor currents

Fig 5.2(b): Rotor current controller

5.2.1 VALUE CALCULATION FOR ROTOR CURRENTS

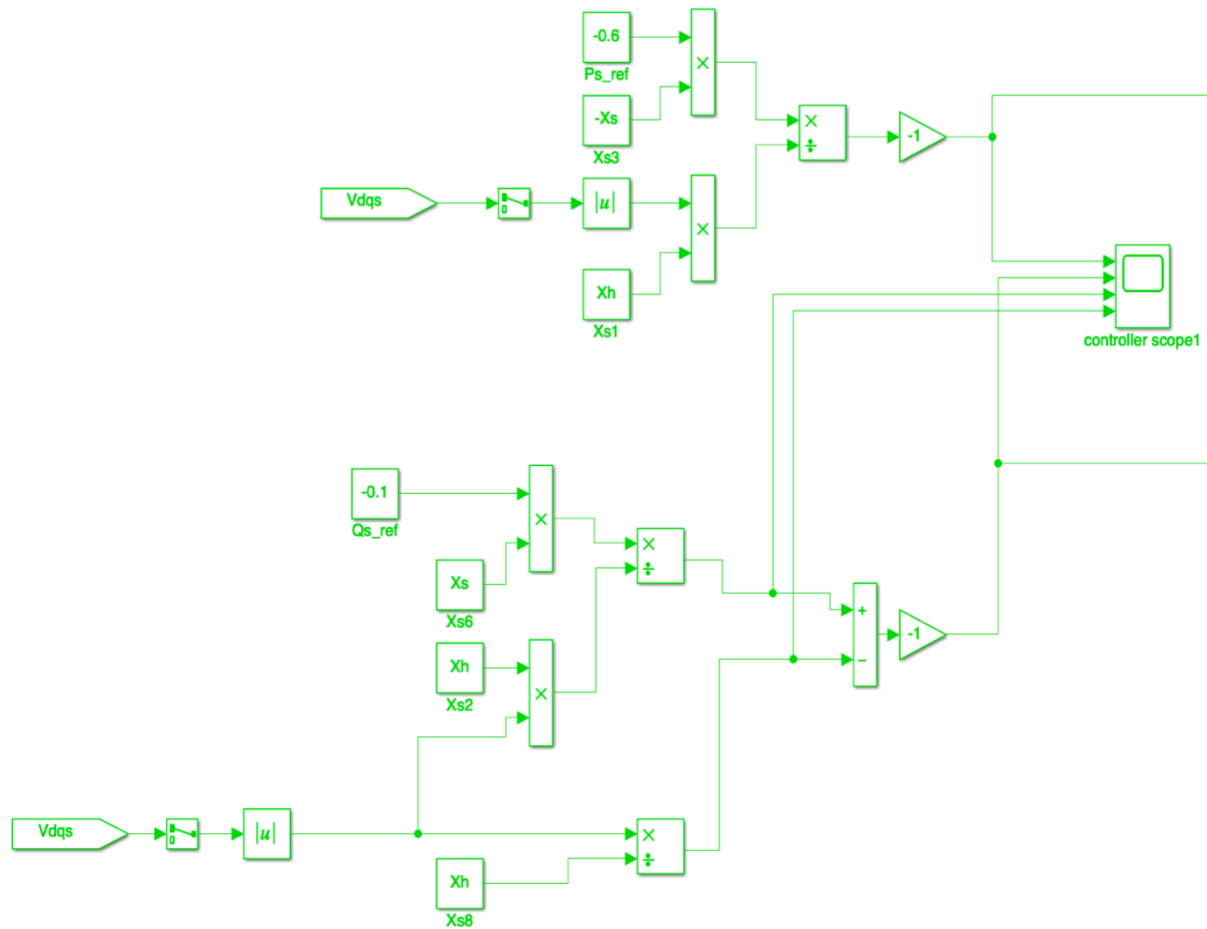


Fig: 5.2(a): Value calculation for rotor currents

From fig 5.1 and fig 5.2(a), we can derive two equations for finding out the d-axis reference current (I_d) and q-axis reference current of the rotor of the DFIG. We must remember that the reference currents depends of the reference values of the active and reactive power of the stator side provided, controlling which we wish to control the stator side active and reactive power flow.

$$-\left(\frac{X_{s3} * P_{s_ref}}{X_s * |V_{dqs}|}\right) = I_{rd_ref} \quad (5.1)$$

$$\left(\frac{XX_s * Q_{s_ref}}{X_s * |V_{dqs}|}\right) - \frac{|V_{dqs}|}{X_h} = I_{rq_ref} \quad (5.2)$$

Equation 1 and 2 are used to find the reference values of d and q axis rotor currents. Using these values of currents we will now move into Rotor current Controller section Fig 5.2(b)

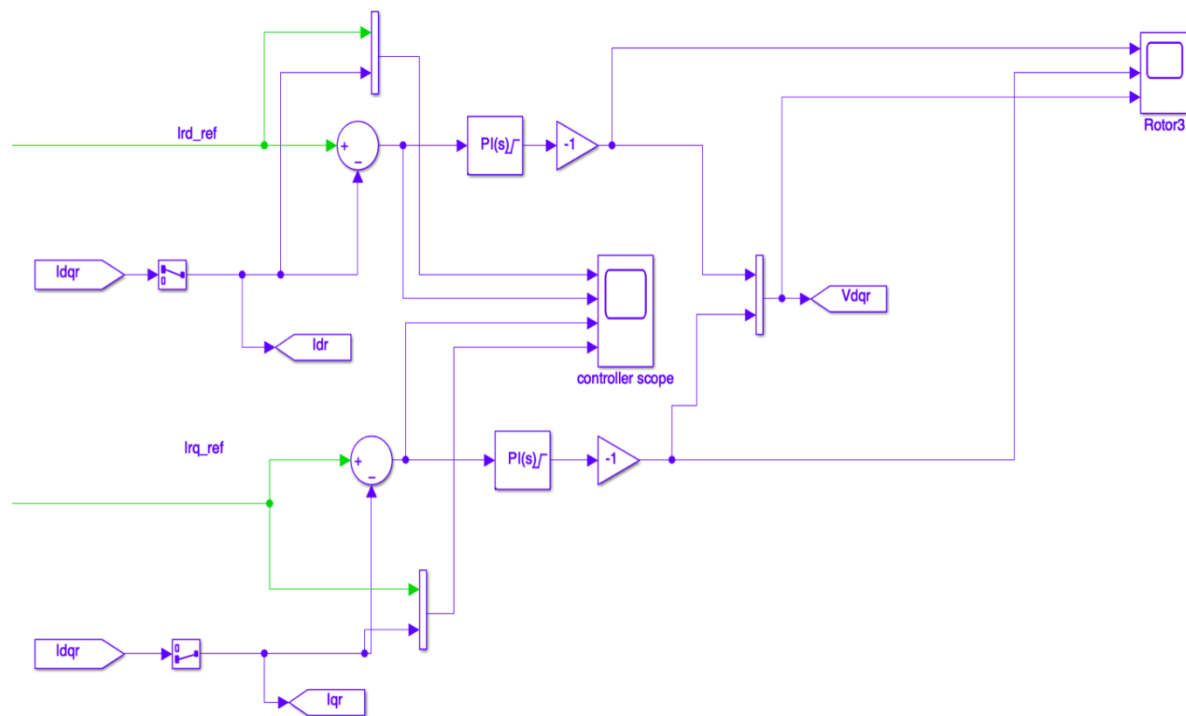


Fig. 5.2(b): Rotor current controller

We will compare the reference currents with the actual rotor current with the use of a comparator and the difference will be fed through a PI controller to obtain d and q axis rotor voltage.

From fig 5.2(b)

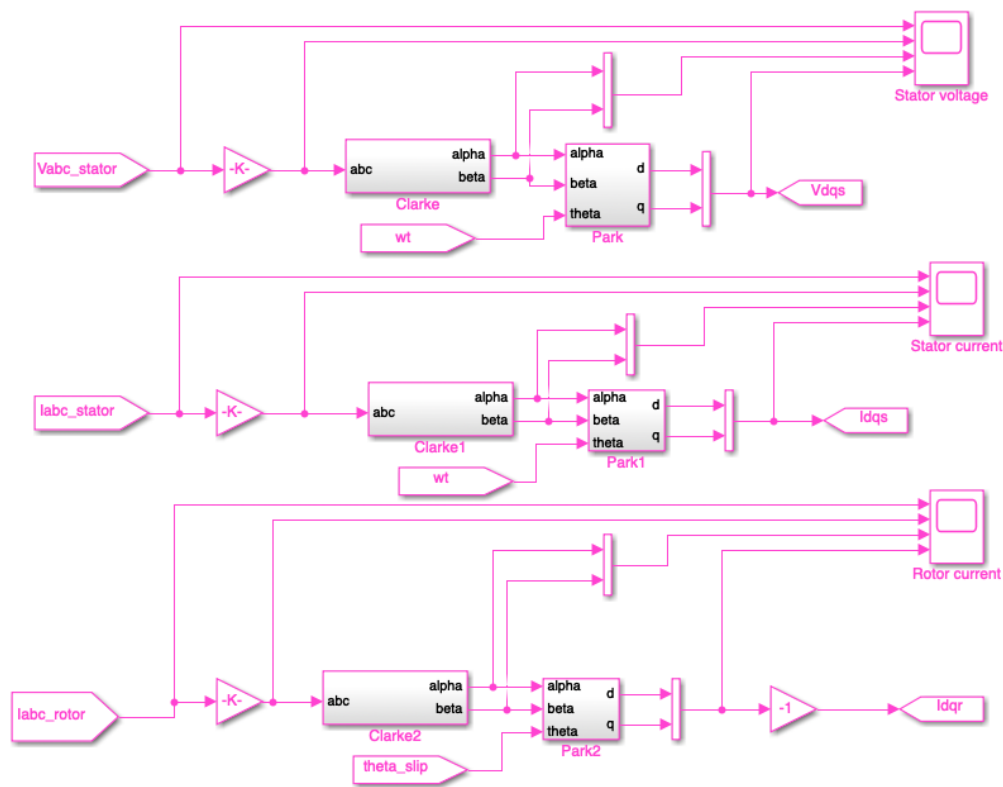
$$V_{dr} = (I_{rd_ref} - I_{dr}) \text{ fed through a PI controller.} \quad (5.3)$$

$$V_{qr} = (I_{rq_ref} - I_{dqr}) \text{ fed through a PI controller.} \quad (5.4)$$

5.2.2 DFIG CONTROL UNIT

The DFIG Control unit consists of not only the RSC Controller but also a Park-Clarke transformation block, which is used to convert a system from 3 phase (a-b-c axis) to 2 phase (d-q axis). The Park-Clarke transformation block is shown in fig 5.3.

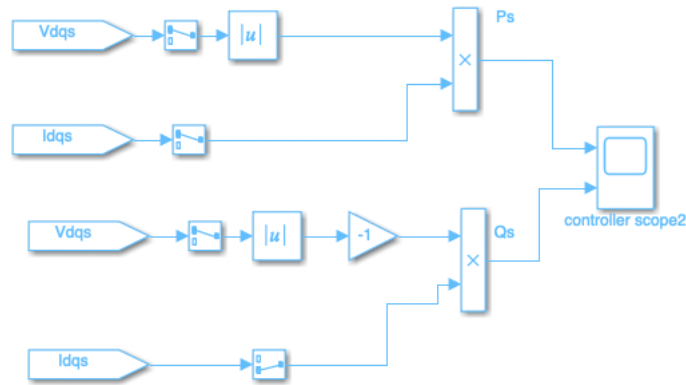
Here 3 phase stator voltage, 3 phase stator and rotor currents are converted into components along d-q axis, which are further used throughout the modelling.



Parks Transformation

Fig. 5.2.2(a): Park Transformation model

Further the DFIG control unit consist of an Active and Reactive Power block shown in fig 5.2.2(b)



Active and reactive power from DFIG

Fig. 5.2.2(b): Active and reactive power calculation model

5.3 ENTIRE DFIG MODELLING

The entire DFIG modelling with the RSC Controller is shown in fig 5.3(a) below.

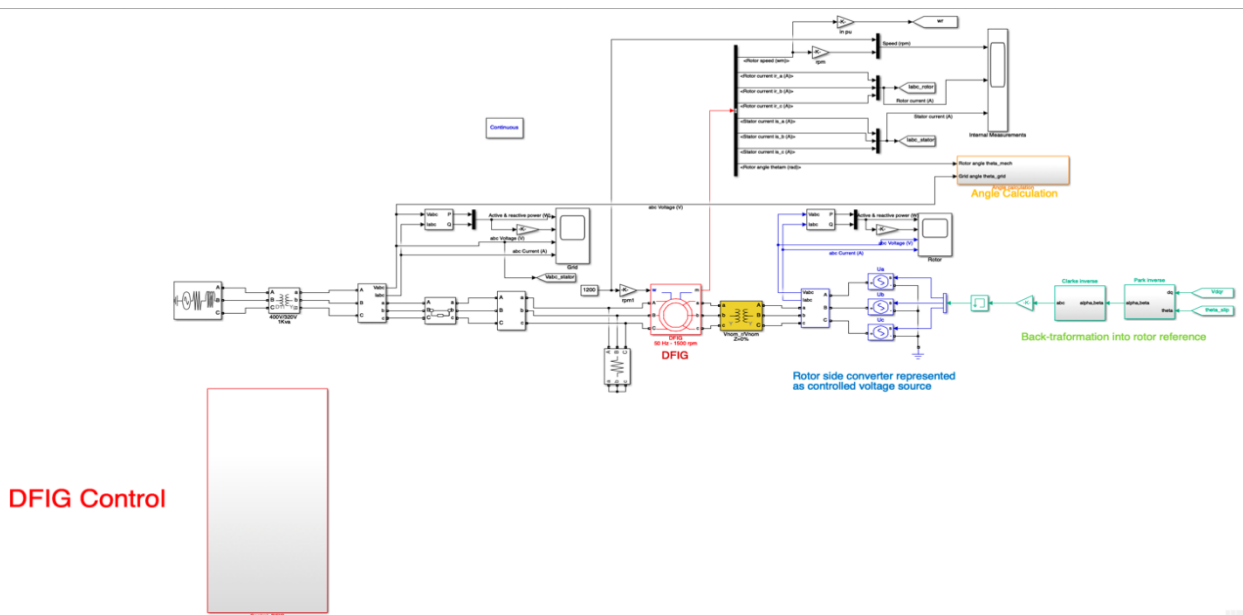


Fig. 5.3(a): Entire DFIG modelling

The DFIG control block is already discussed above. Here we are going to discuss about the main body. It is divided into 2 sections for better understanding

Fig 5.3.1(a): The stator side of the DFIG

Fig 5.3.2(a): The Rotor side of the DFIG

5.3.1 THE STATOR SIDE OF THE DFIG

The model for the stator side of the DFIG is shown in fig 5.6(a)

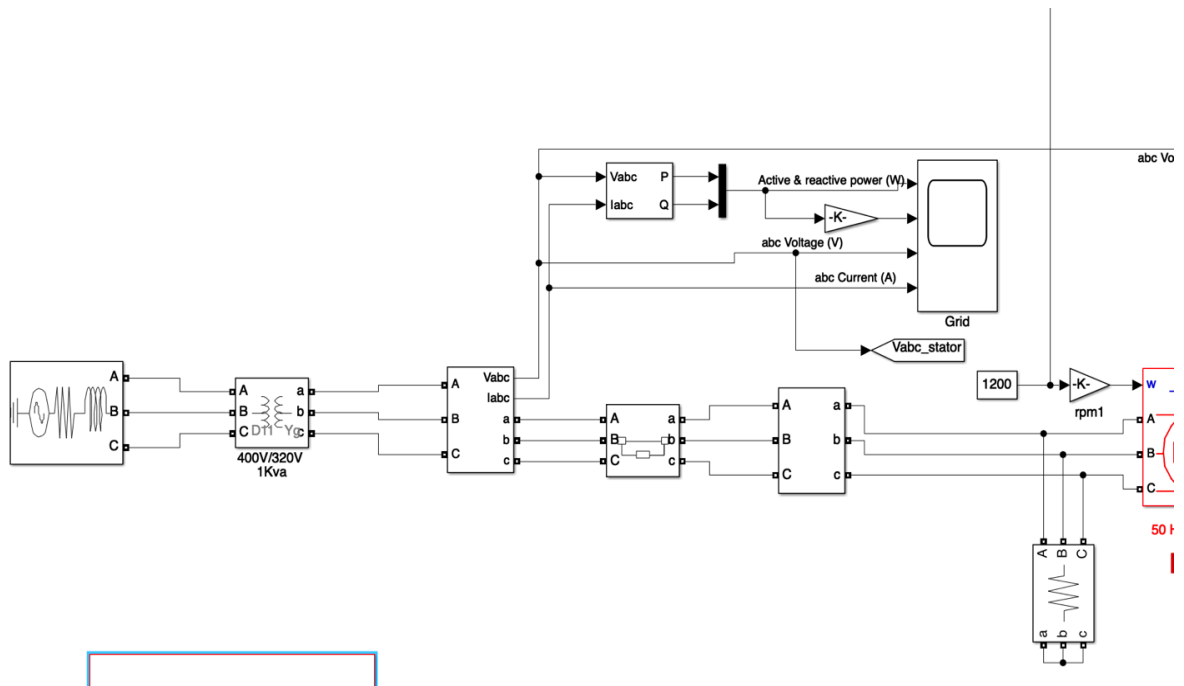


Fig. 5.3.1(a): The stator side of the DFIG

Here we find that the stator of the DFIG is fed from a Source through a step-down transformer.

The source reading are as follows: Phase-to-phase voltage (V_{ph_rms})= 400V, 50Hz. The line resistance in the stator side is $5M\Omega$ has been put through a block. We find V_{abc_stator} directly from this model and putting V_{abc_stator} and I_{abc_stator} through the 3 phase instantaneous power measurement block gives us the stator active and reactive power.

The DFIG is shown in fig 5.6(b). It is 50 Hz and maximum rated speed is 1500 rpm. We provide default speed of 1200 rpm to the generator and multiply it with $(2*\pi)/60$ to make it rad/s.

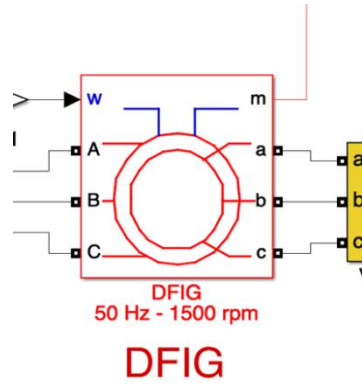


Fig. 5.3.1(b): DFIG Block

The respective values of the 3 phase stator and rotor currents and the Rotor speed, rotor angle are taken from the measurement terminal of the DFIG block as shown in fig 5.6(b). All the stator current values are taken into a 3*1 stator current mux and the rotor current values are taken into another 3*1 rotor current mux as shown in fig 5.6(c). The values of stator current (I_{abc_stator}) and rotor current (I_{abc_rotor}) are saved for future references and calculations.

The values of 3 phase stator current, rotor current and rotor speed (in rpm) are taken into internal measurement block, as shown in fig 5.3.1(c).

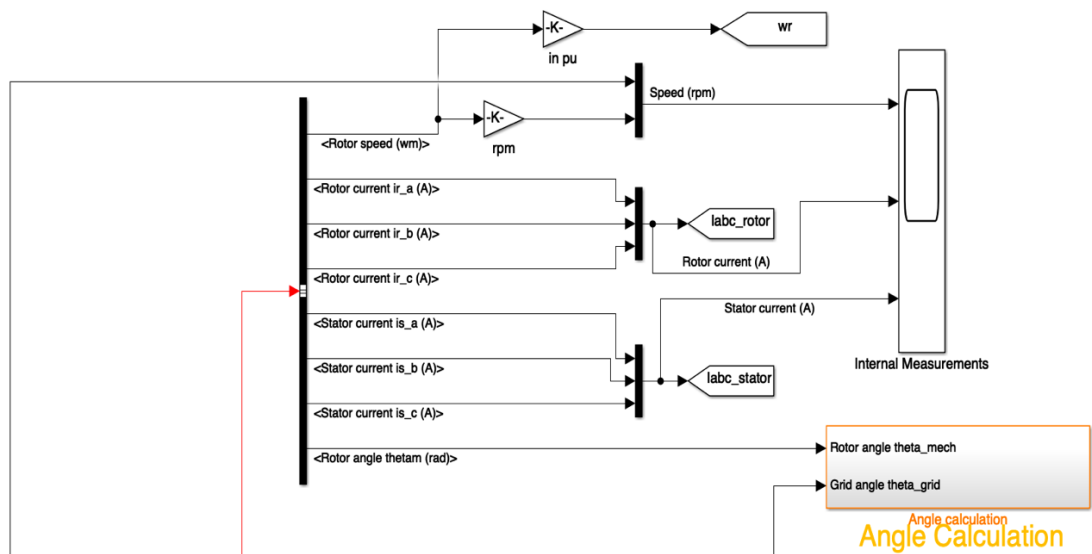


Fig. 5.3.1 (c): Model for finding speed and 3 phase stator and rotor currents

There is another block called the angle calculation block. The inputs to this block are the rotor angle in radian and the three phase stator voltage (Shown in Fig 5.3.1(d))

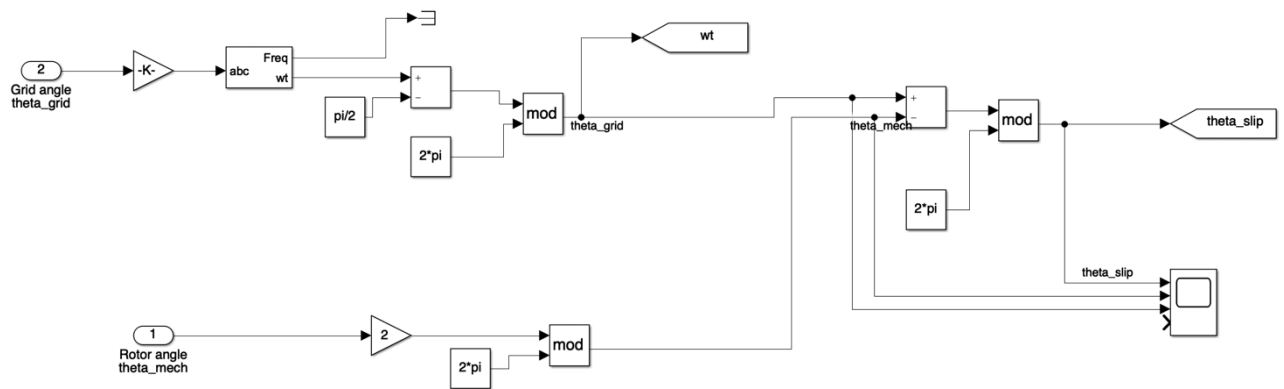


Fig. 5.3.1(d): Angle Calculation block

From fig 5.6(d), we find that the value of the 3 phase stator voltage is taken into input 2 of the angle calculation block, which is multiplied with a multiplier K and fed into a PLL block.

The value of K is $\frac{\sqrt{3}}{(\sqrt{2} * 320)}$

The 3 phase stator voltage then is passed through a Phase Locked Loop (PLL) block, the function of this block is to take voltage as input, and send frequency and angle (ωt) as output. For the stator phase voltage angle we provide a shift of $\pi/2$

This is then passed through a mod block, the function of which is to divide input 1 by input 2 and provide the remainder as output.

Hence for input 2: $\frac{(\omega t - \pi/2)}{2\pi}$ the remainder of which is the stator or the grid angle ωt . We want to find at any instant how much the stator angle is more or less than 2π , and that value determines the stator or the grid angle. Hence we take the mod block.

Similarly the rotor angle follows a similar process to find the rotor angle.

Finally the difference between the stator and the rotor angle gives us the value of slip angle θ_{slip} .

θ_{slip} and ωt are kept stored for future use in the MATLAB model.

5.3.2 THE ROTOR SIDE OF THE DFIG

The MATLAB model for the rotor side of the DFIG is given in figure 5.3.2(a)

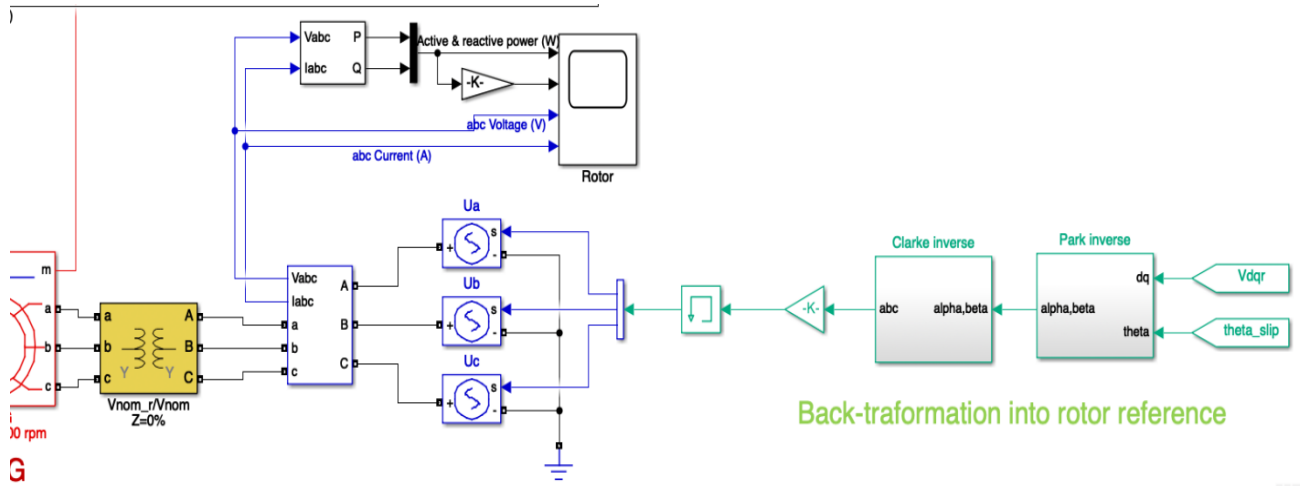


Fig. 5.3.2(a): The Rotor side of the DFIG

We can here observe back transformation of the rotor reference. θ_{slip} is obtained from the angle calculation block and V_{dqr} is obtained from the DFIG control block as shown earlier.

Here we put both the parameters through inverse Park and Clarke transformation, to obtain 3 phase rotor voltages.

The 3 phase rotor voltages are multiplied by a factor (constant)= K and fed through a memory block. The rotor voltages are given as an input to the rotor side of the DFIG, and rotor voltage (V_{abc}) and current (I_{abc}) are given as input to the power block to find the rotor active and reactive power.

Inverse Park Transformation:

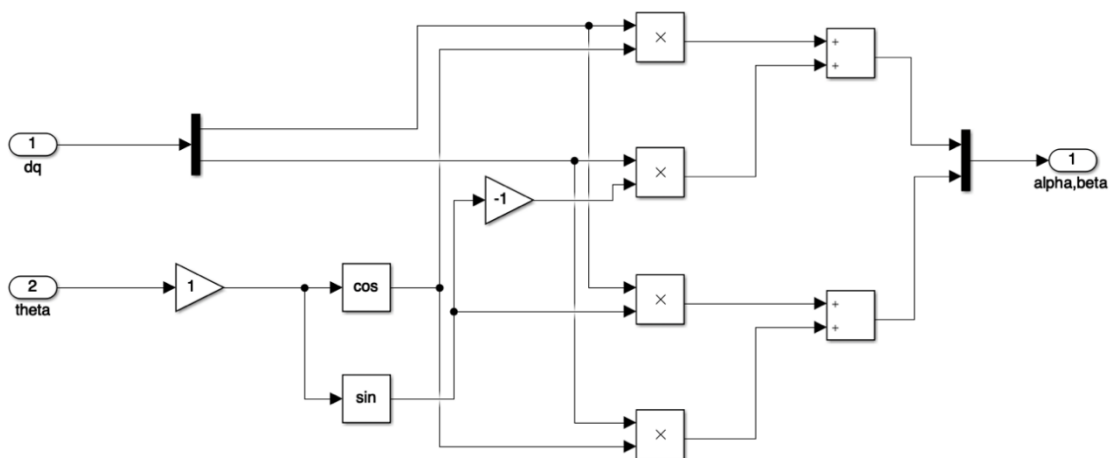


Fig. 5.3.2(b): Inverse Park Transformation block

CHAPTER 6

RESULTS AND OBSERVATIONS

Here, we start to find the stator active and reactive power by changing the per unit values of reference values of stator powers.

NOTE

- The fig a shows the complete profile, fig b shows the initial transient value, and the fig c shows the final steady state value.
- The red curve shows the active power and the blue curve shows the reactive power.
- Here we analyse 4 curves: active and reactive power, active and reactive power in pu, 3 phase stator voltage and 3 phase stator current
- We consider 1 case: for speed 1200 rpm

6.1 Sub-synchronous case of rotor Speed = 1200 rpm

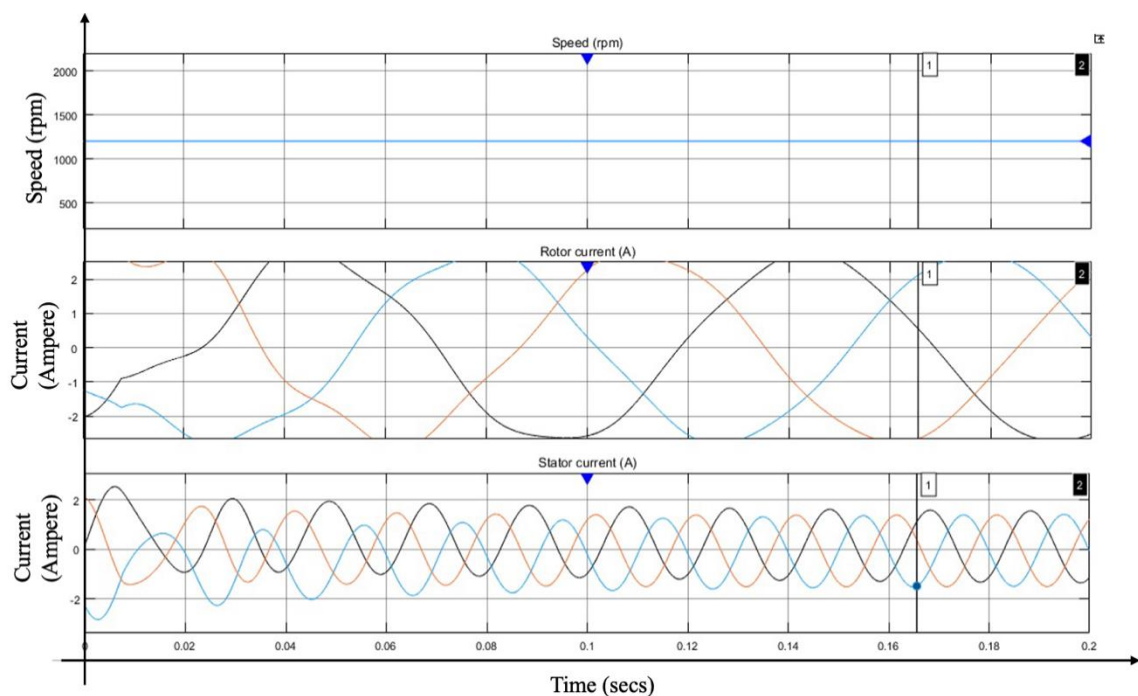


Fig. 6.1

6.1.1 CASE 1: $P_S = -0.2$ p.u. $Q_S = -0.9$ p.u.

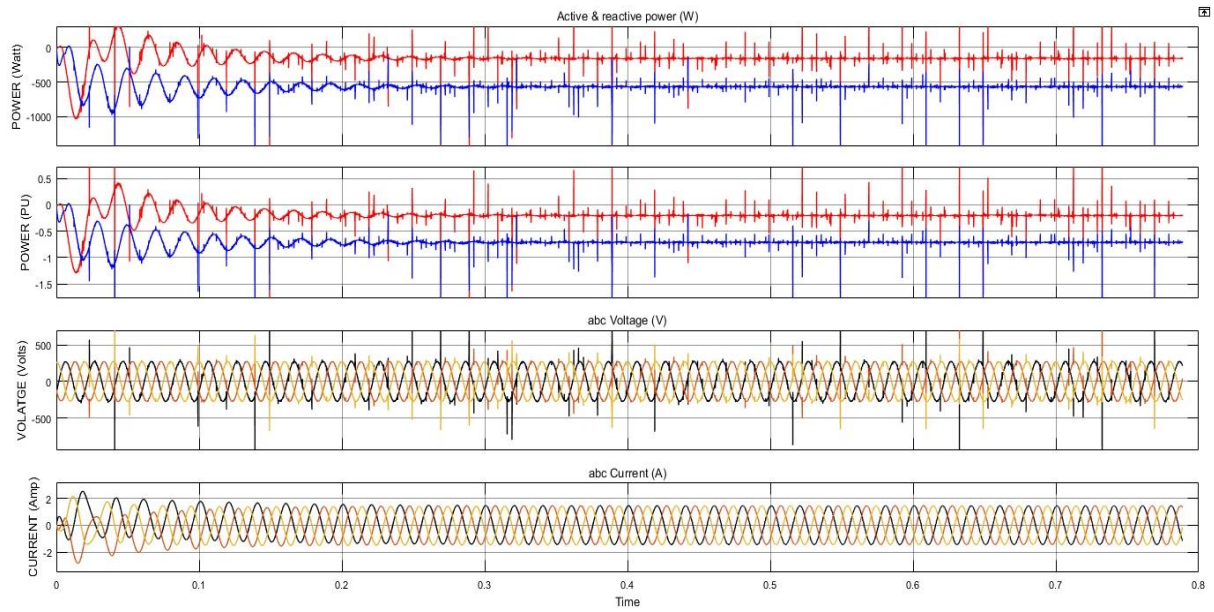


Fig. 6.1.1(a)

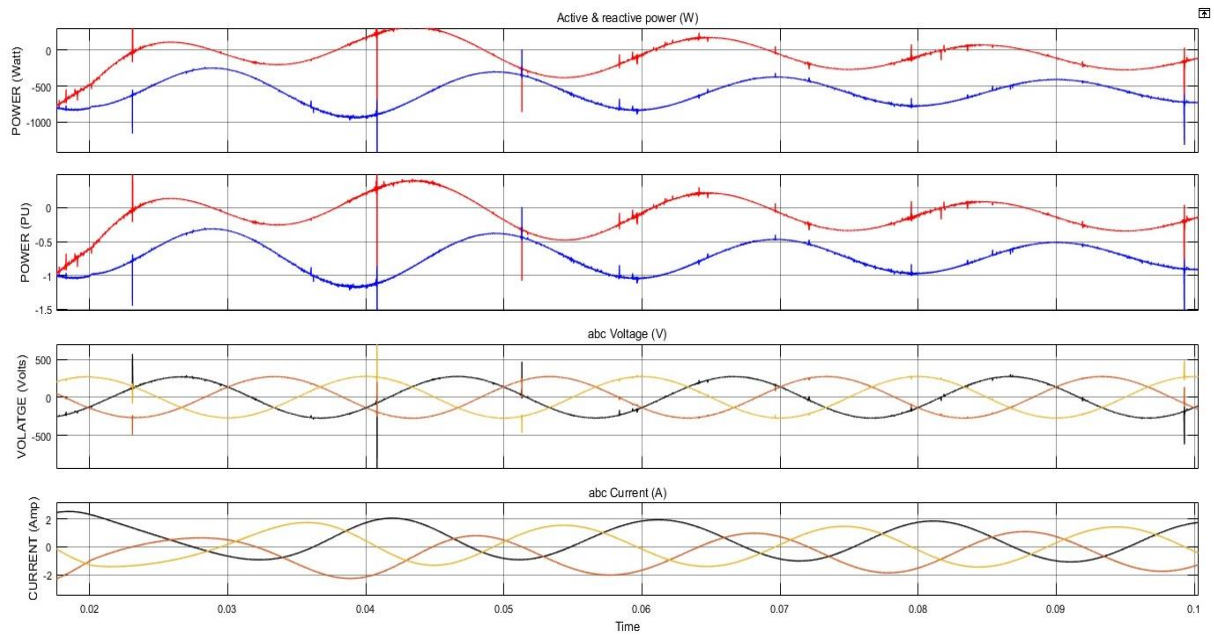


Fig. 6.1.1(b)

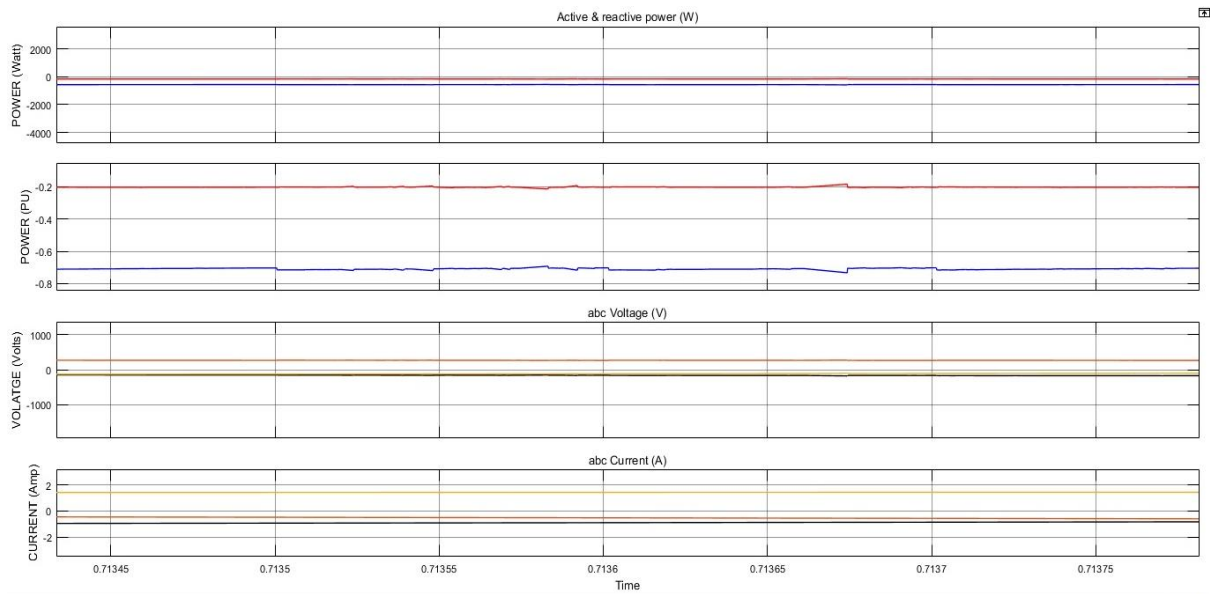


Fig. 6.1.1(c)

- The fig a shows the complete profile, fig b shows the initial transient value, and the fig c shows the final steady state value. The time is taken in seconds.
- The red curve shows the active power and the blue curve shows the reactive power.
- The active power curve matches with the reference active power of 0.2 pu but there is some differences in reactive power.

6.1.2 CASE 1: $P_s = -0.3$ p.u. $Q_s = -0.8$ p.u.

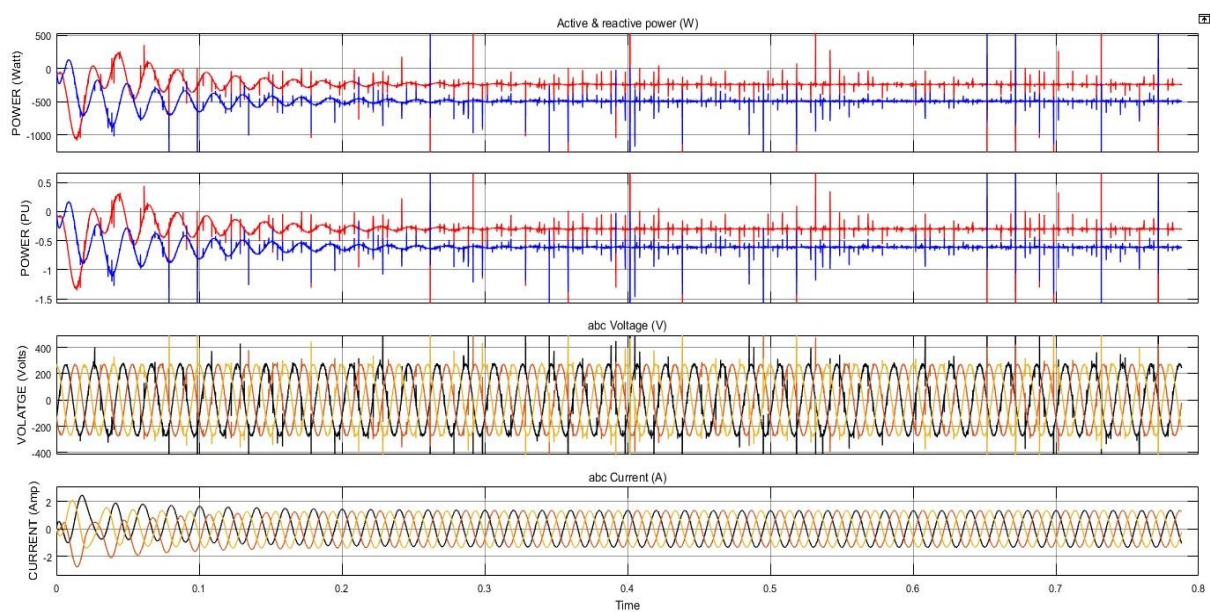


Fig. 6.1.2(a)

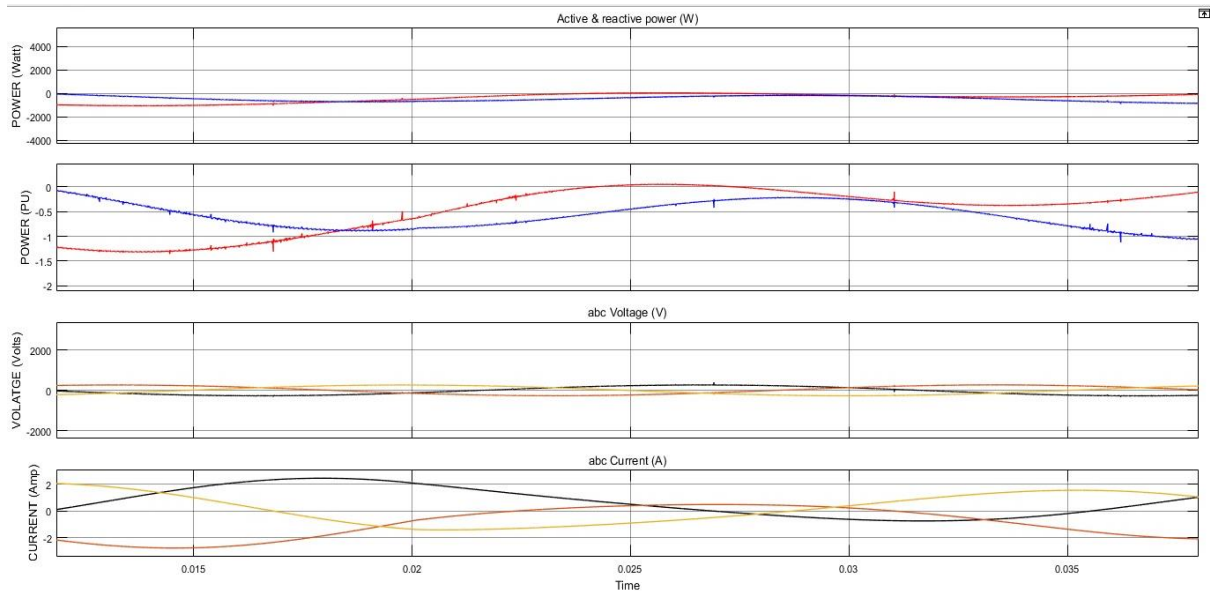


Fig. 6.1.2(b)

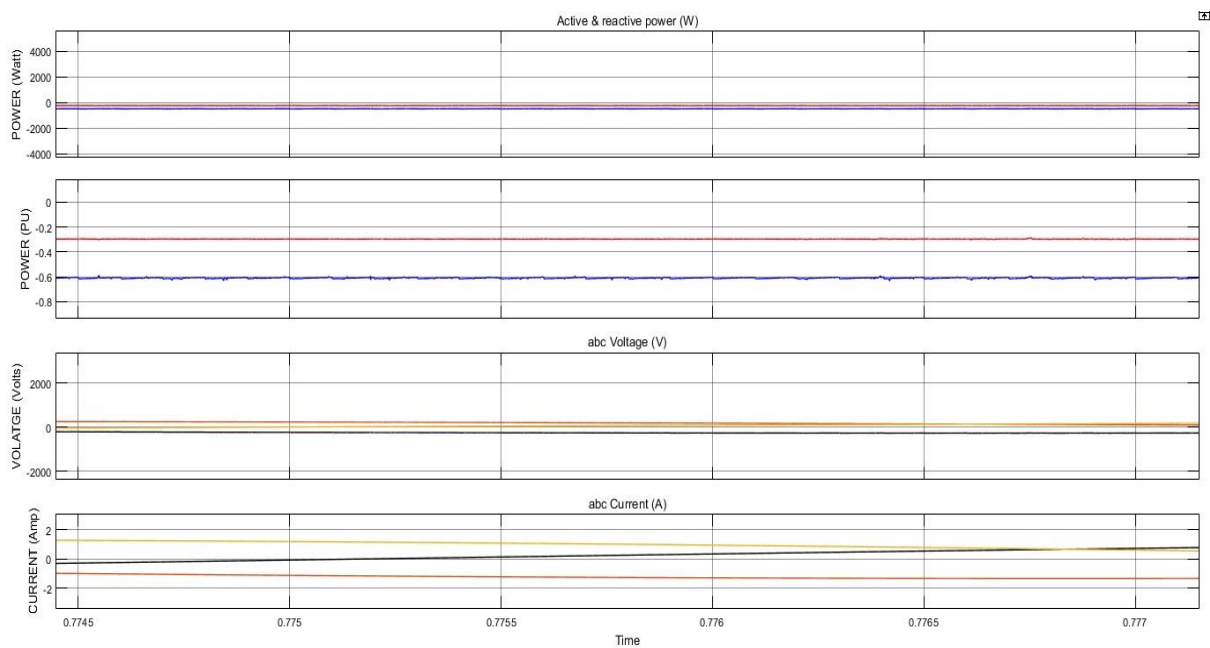


Fig. 6.1.2(c)

- The fig a shows the complete profile, fig b shows the initial transient value, and the fig c shows the final steady state value. The time is taken in seconds
- The red curve shows the active power and the blue curve shows the reactive power.

- The active power curve matches with the reference active power of 0.3 pu but there is some differences in reactive power.
- The reactive power differs from the reference value by almost 0.2 pu

6.1.3 CASE 3: $P_S = -0.4$ p.u. $Q_S = -0.7$ p.u.

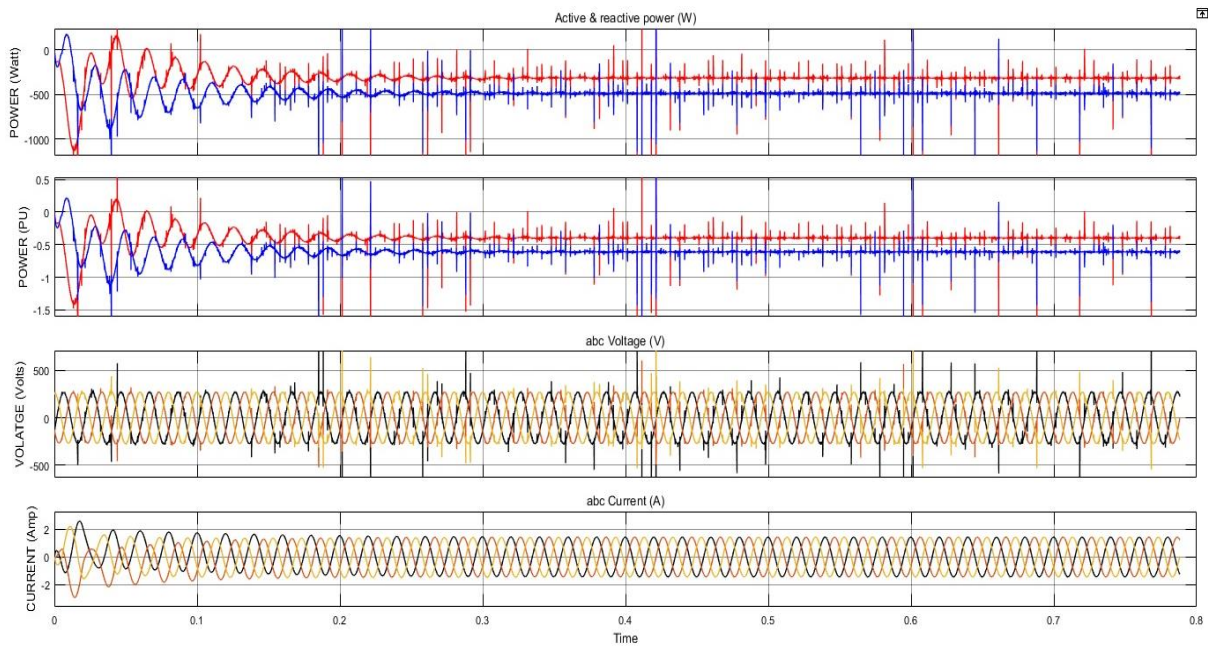


Fig. 6.1.3(a)

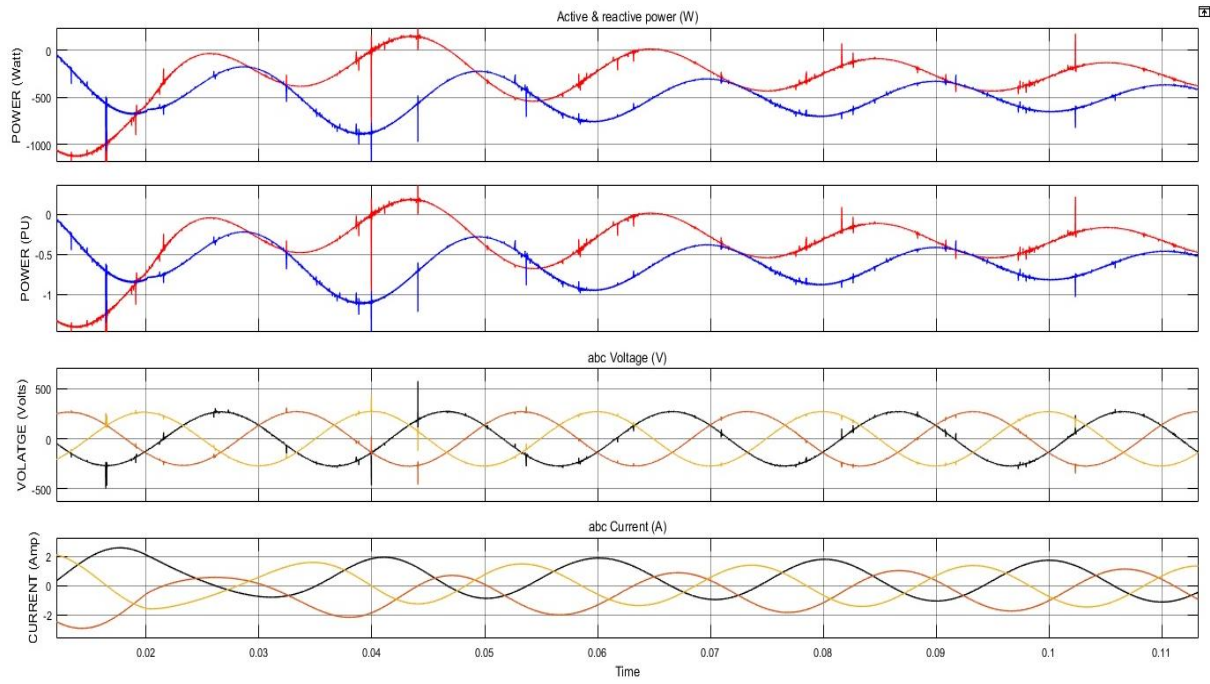


Fig. 6.1.3(b)

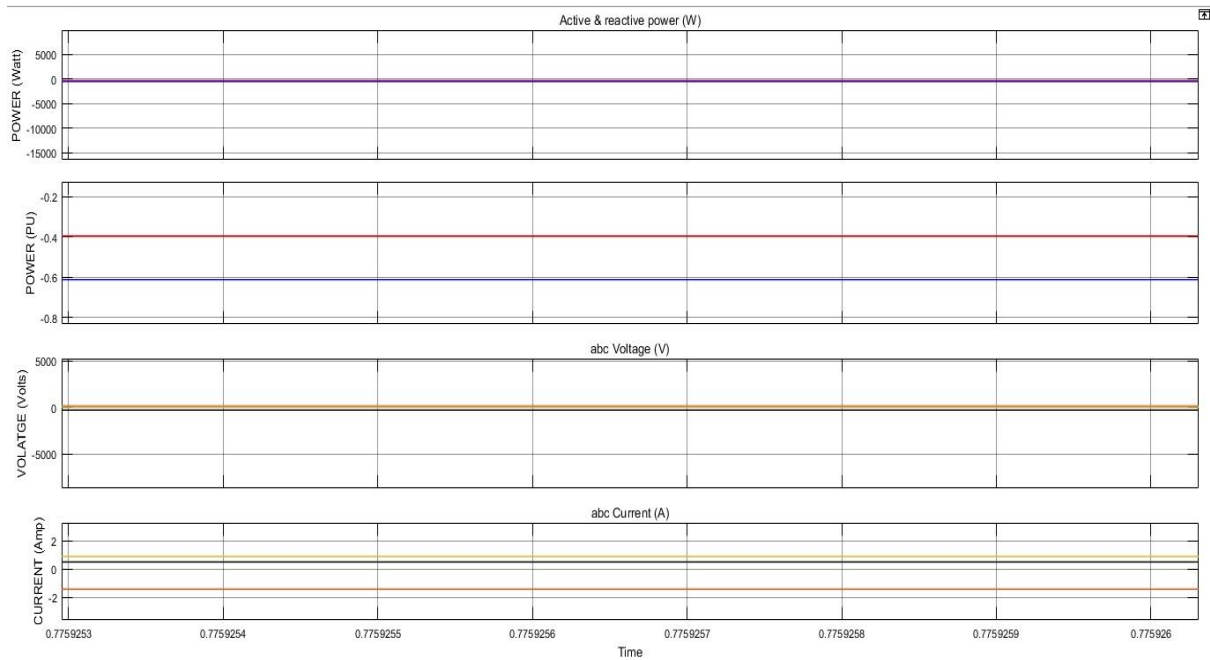


Fig. 6.1.3(c)

- The fig a shows the complete profile, fig b shows the initial transient value, and the fig c shows the final steady state value. The time is taken in seconds
- The red curve shows the active power and the blue curve shows the reactive power.
- The active power curve matches with the reference active power of 0.4 pu but there is some differences in reactive power by almost 0.08 units
- This difference in reactive power is minimum

6.1.4 CASE 3: $P_S = -0.9$ p.u. $Q_S = -0.3$ p.u.

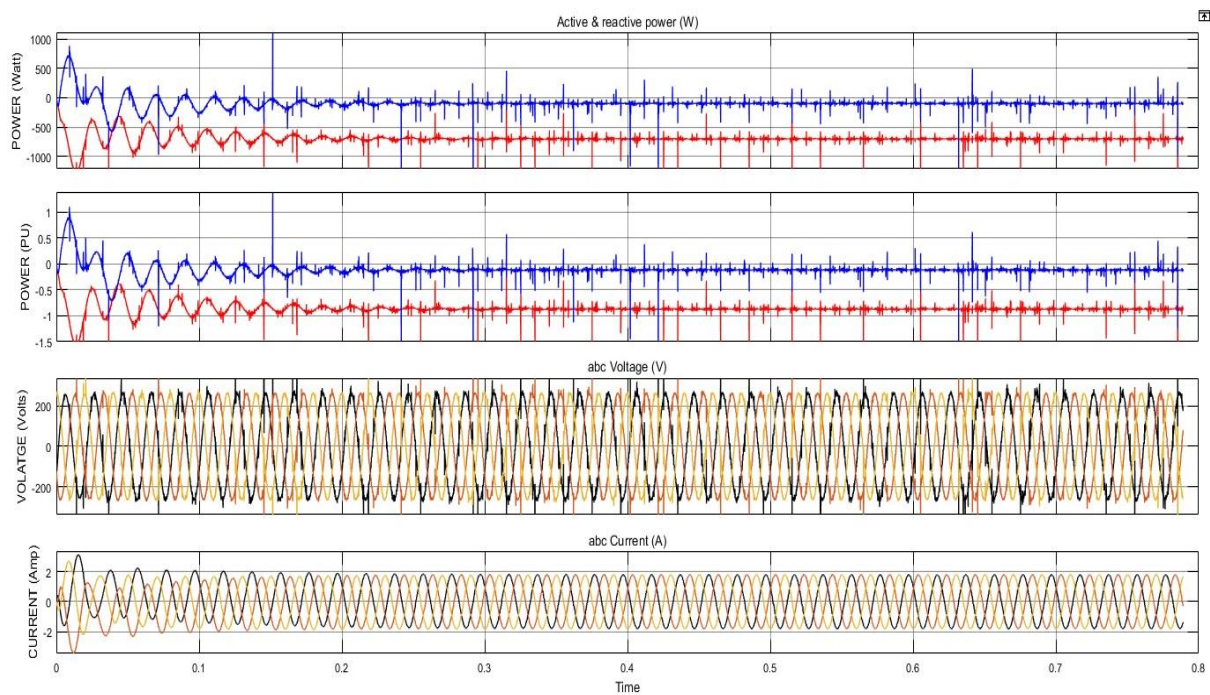


Fig. 6.1.4(a)

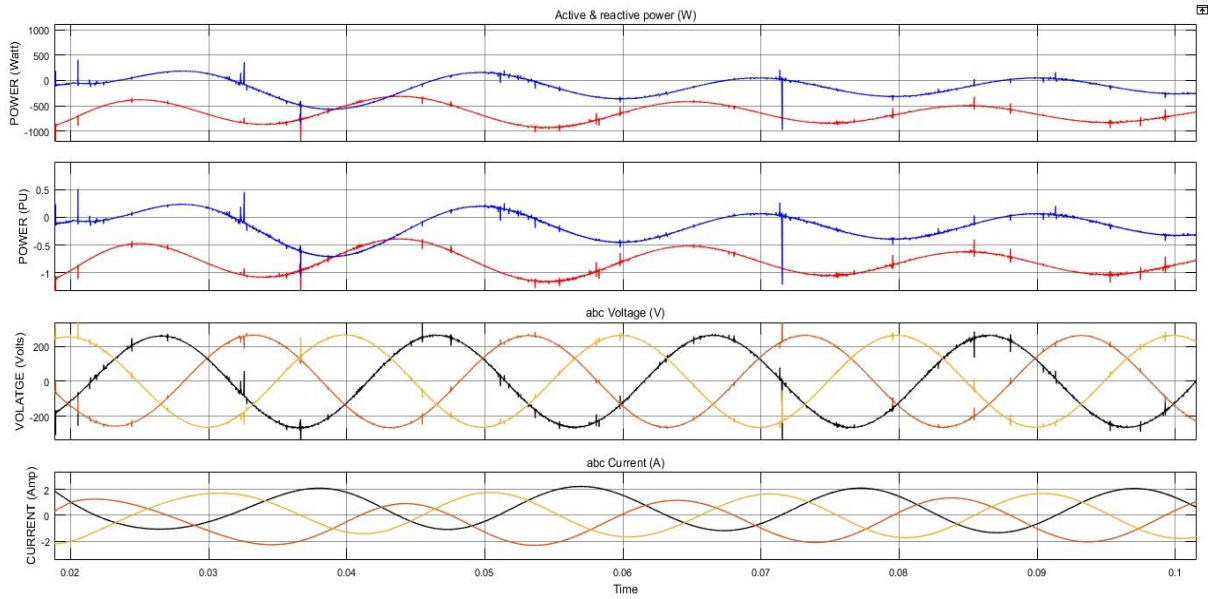


Fig. 6.1.4(b)

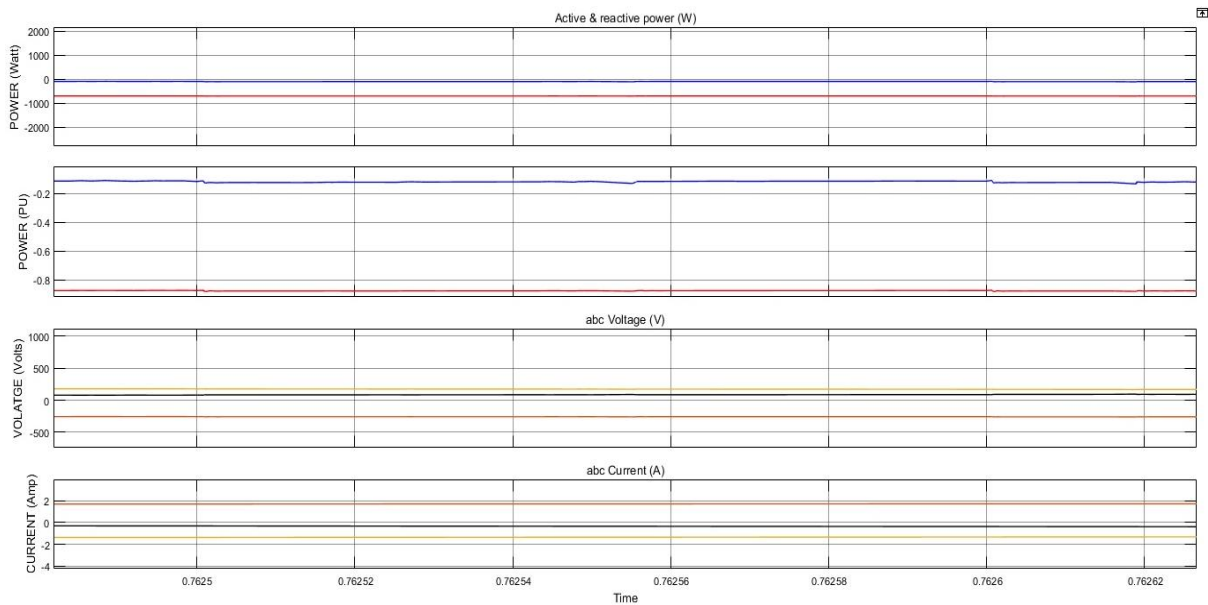


Fig. 6.1.4(c)

- The fig a shows the complete profile, fig b shows the initial transient value, and the fig c shows the final steady state value. The time is taken in seconds
- The red curve shows the active power and the blue curve shows the reactive power.
- The active power curve matches with the reference active power of 0.9 pu but there is some differences in reactive power by 0.19 pu

6.1.5 CASE 5: $P_S = -0.8$ p.u. $Q_S = -0.4$ p.u.

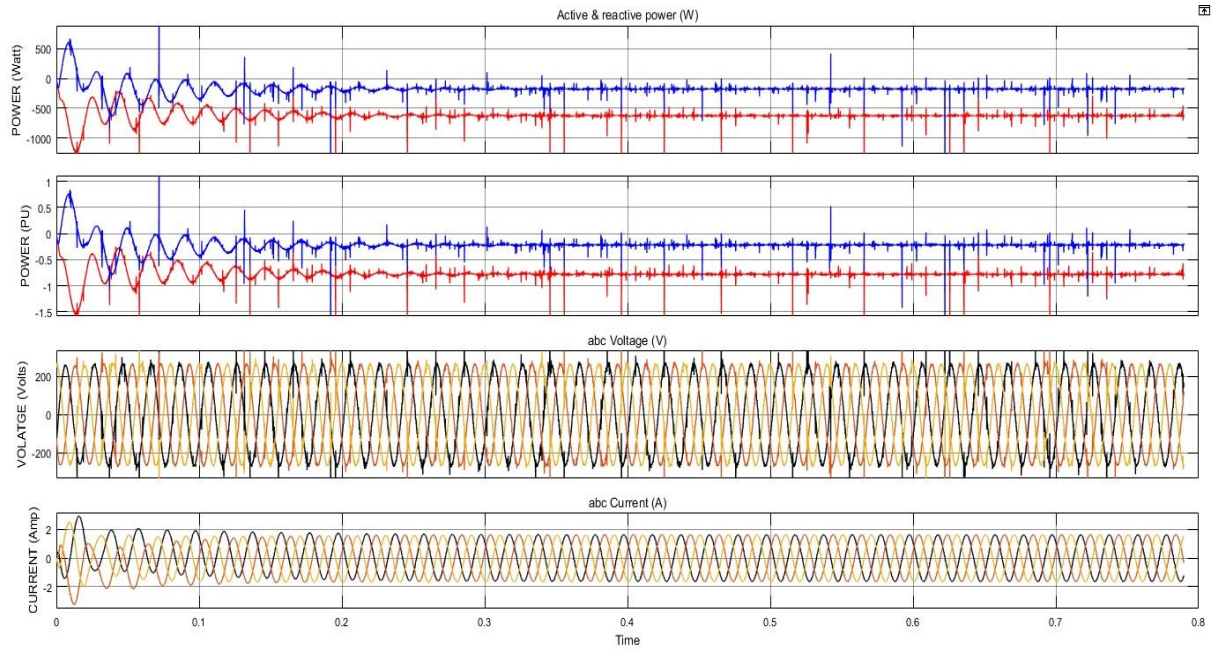


Fig. 6.1.5(a)

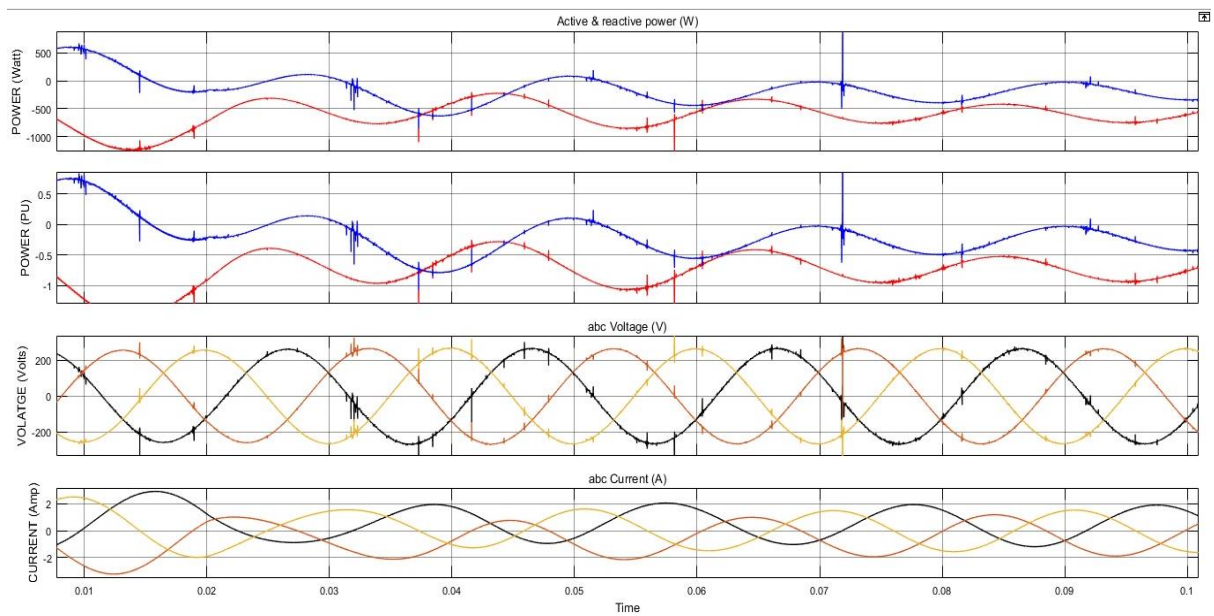


Fig. 6.1.5(b)

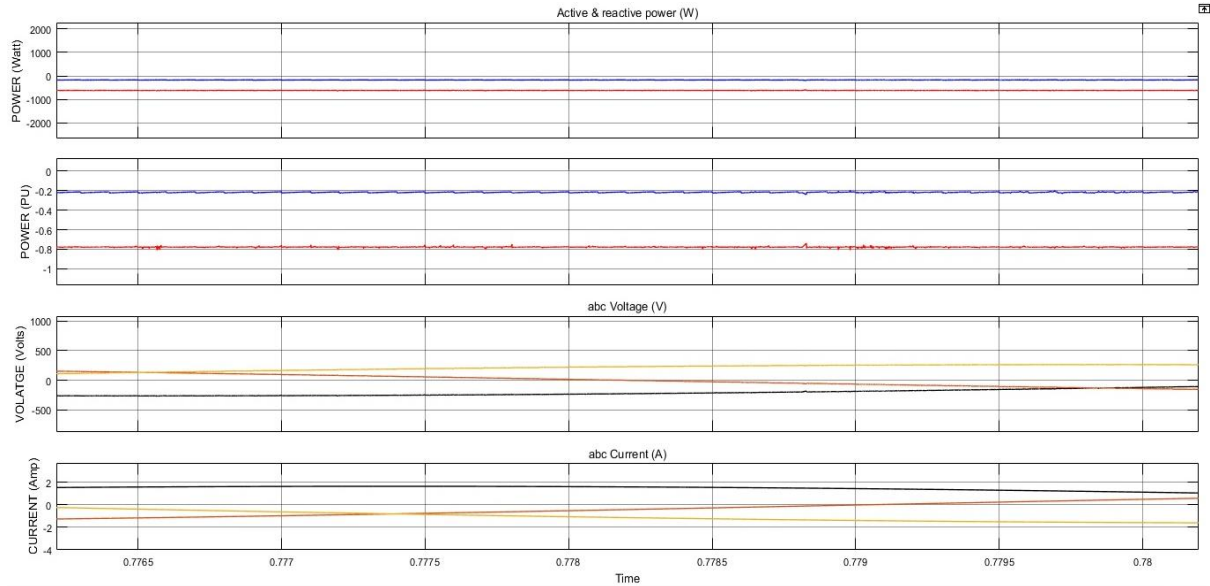


Fig. 6.1.5(c)

- The fig a shows the complete profile, fig b shows the initial transient value, and the fig c shows the final steady state value. The time is taken in seconds
- The red curve shows the active power and the blue curve shows the reactive power.
- The active power curve matches with the reference active power of 0.8 pu but there is some differences in reactive power by 0.19 pu

6.1.6 CASE 6 $P_s = -0.7$ p.u. $Q_s = -0.3$ p.u.

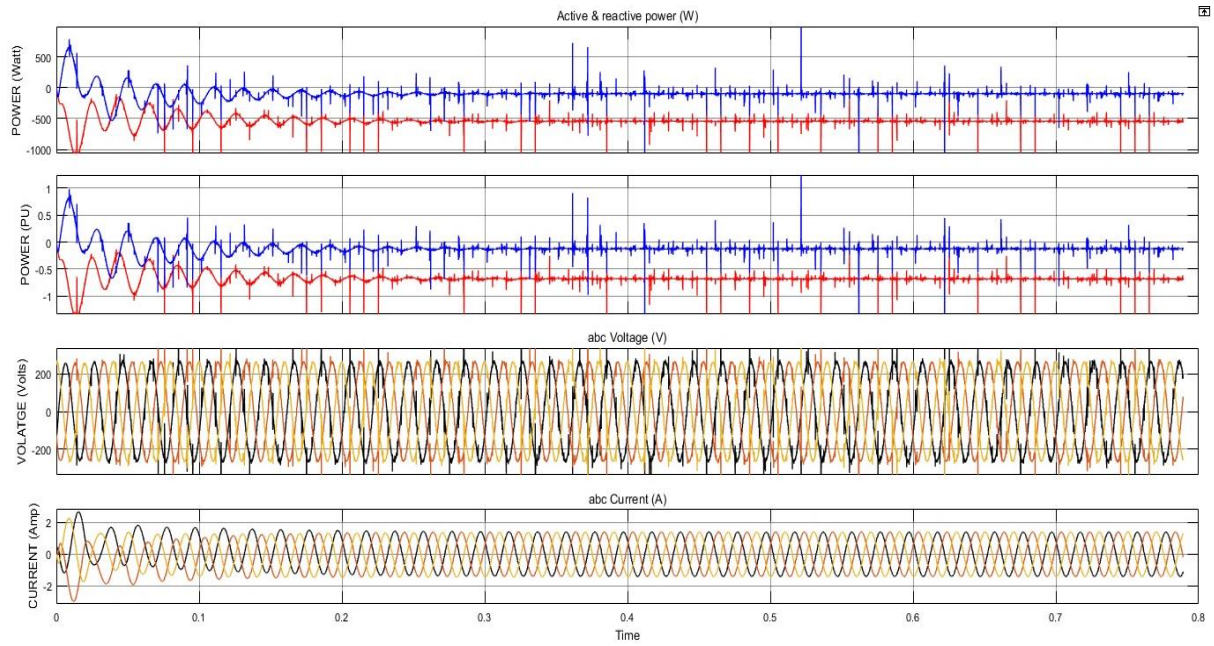


Fig. 6.1.6(a)

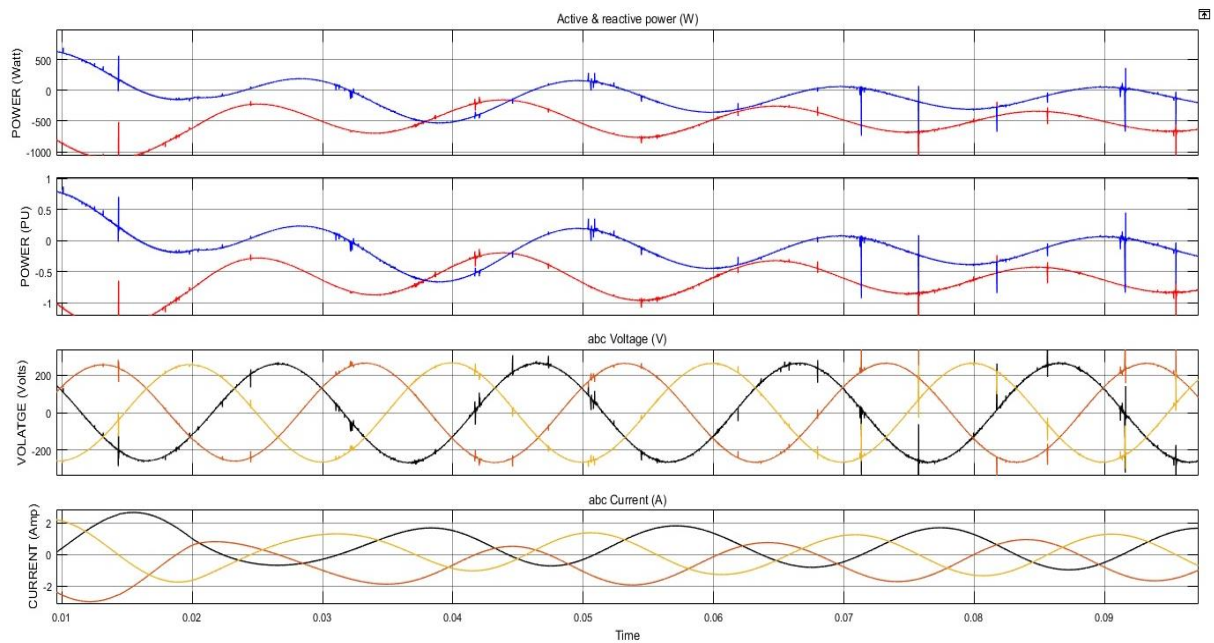


Fig. 6.1.6(b)

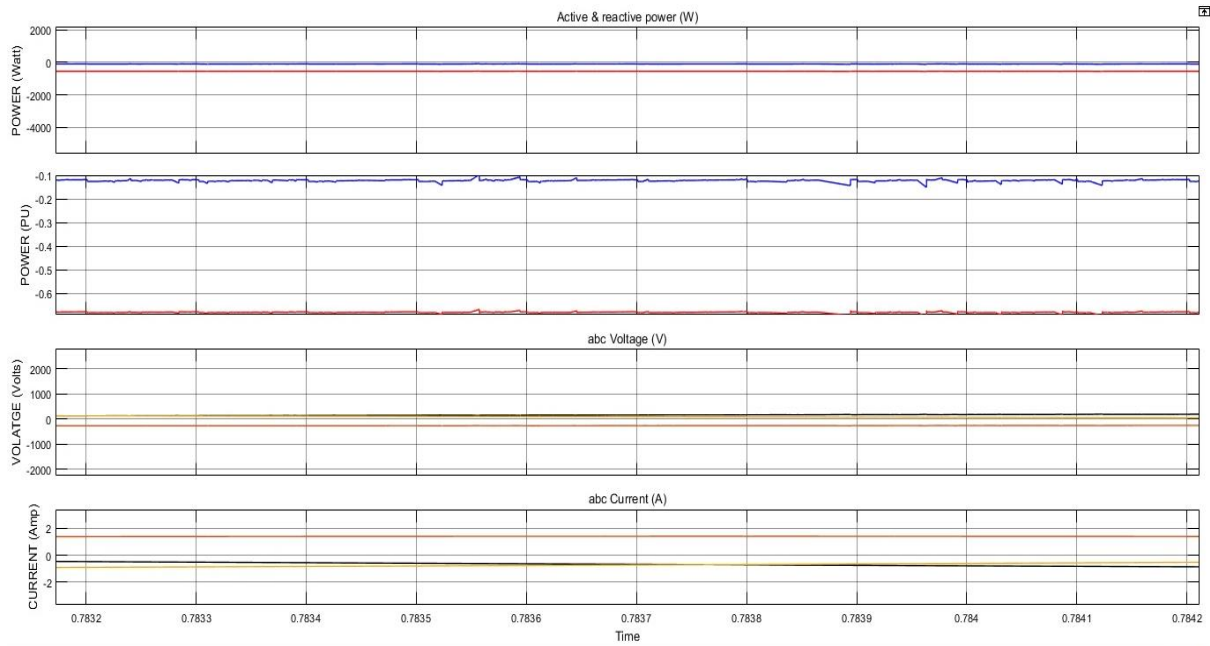


Fig. 6.1.6(c)

- The fig a shows the complete profile, fig b shows the initial transient value, and the fig c shows the final steady state value. The time is taken in seconds
- The red curve shows the active power and the blue curve shows the reactive power.
- The active power curve matches with the reference active power of 0.7 pu but there is some differences in reactive power by 0.17 pu
- There is a slight reduction in difference value of reactive power for this case but the minimum difference value remains case no 3.

6.2 Super-Synchronous case of rotor speed =1700 rpm

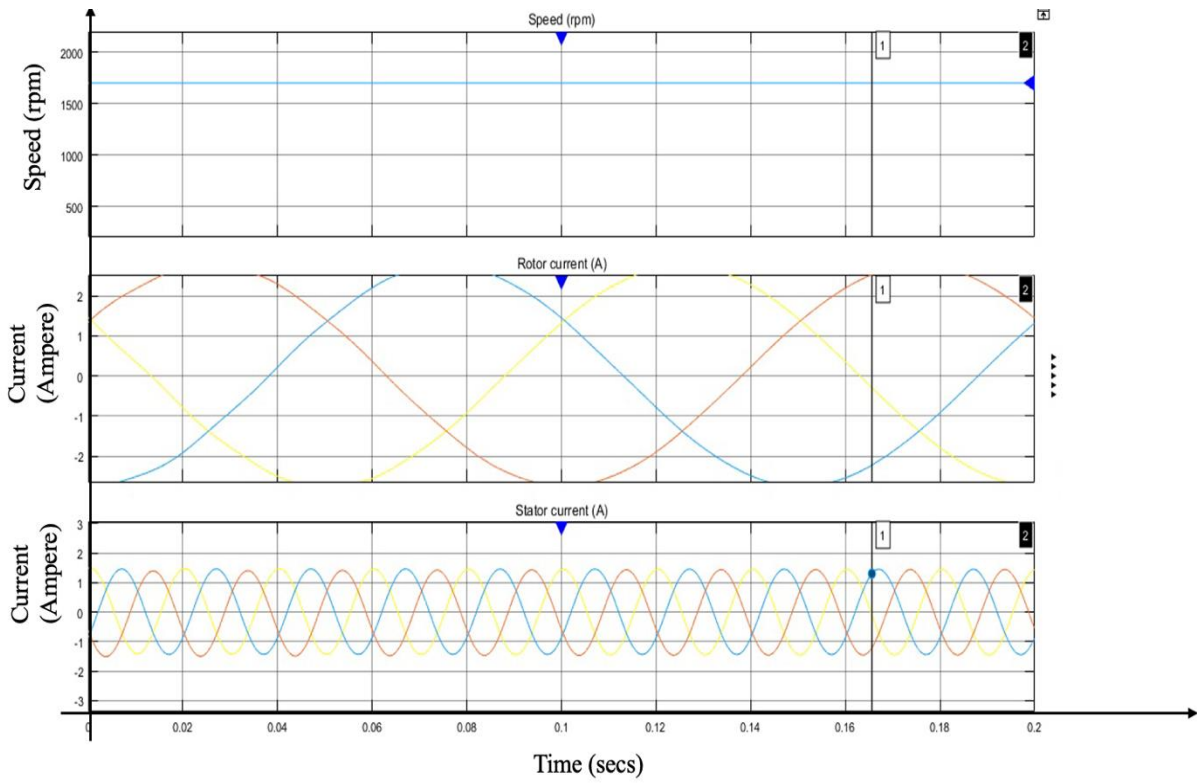


Fig 6.2

6.2.1 CASE 1: $P_S = -0.2$ p.u. $Q_S = -0.9$ p.u.

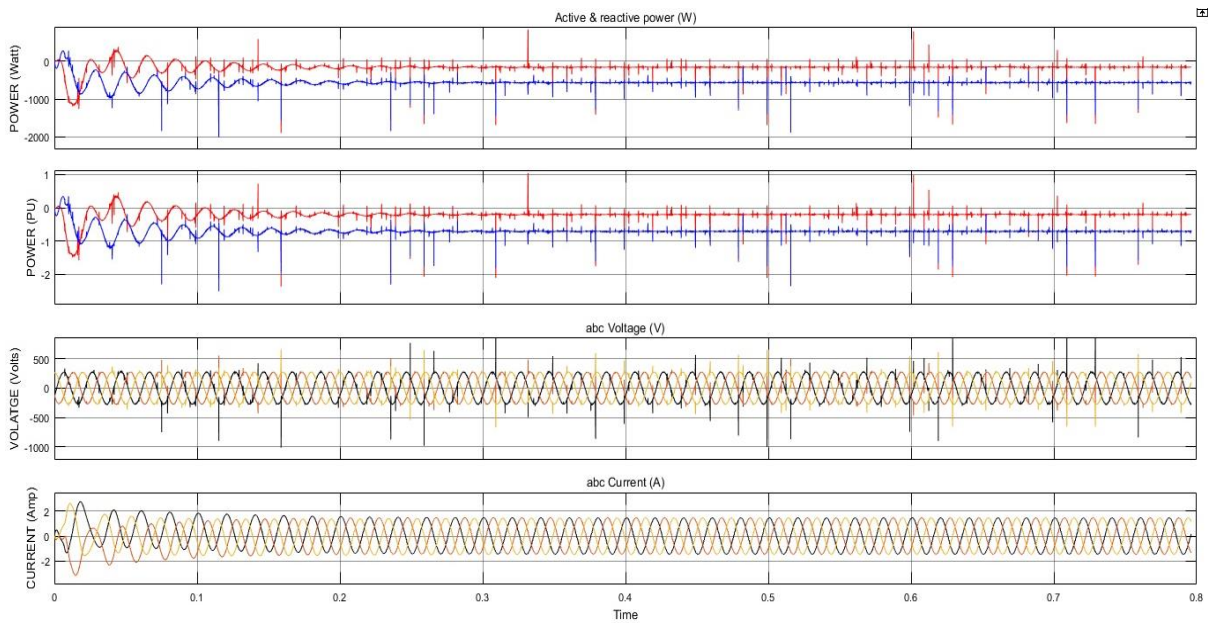


Fig 6.2.1 (a)

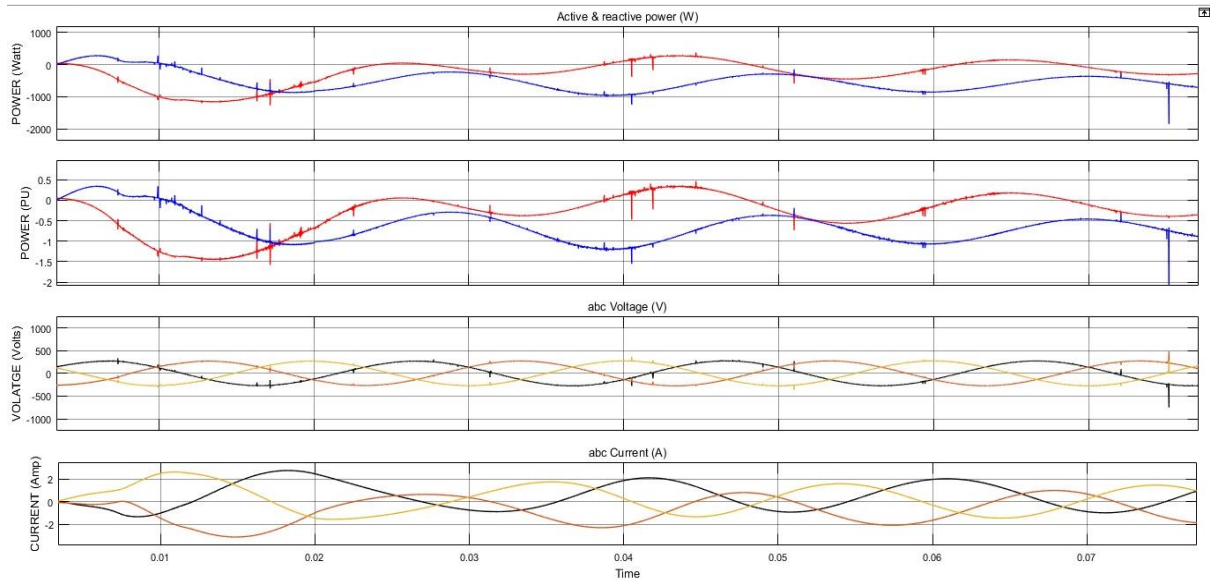


Fig 6.2.1 (b)

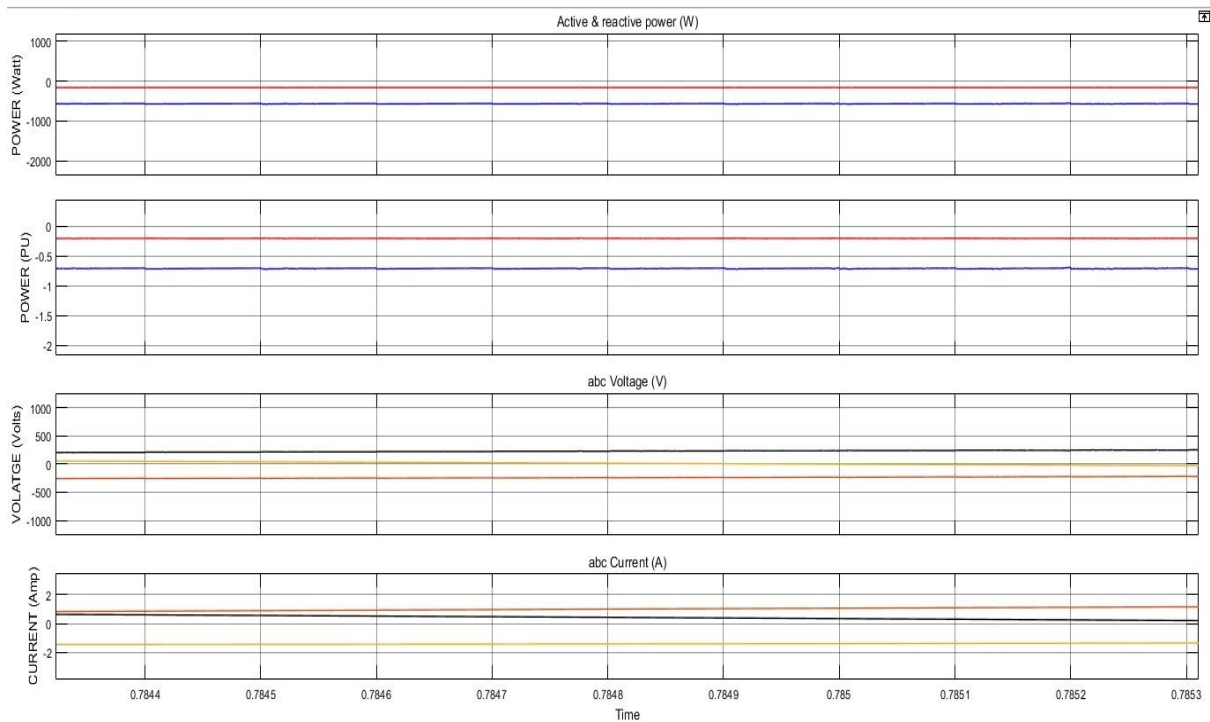


Fig 6.2.1 (c)

- The fig a shows the complete profile, fig b shows the initial transient value, and the fig c shows the final steady state value. The time is taken in seconds
- The red curve shows the active power and the blue curve shows the reactive power.

- The active power curve matches with the reference active power of 0.2 pu but there is some differences in reactive power.

6.2.2 CASE 2: $P_s = -0.8$ p.u. $Q_s = -0.4$ p.u.

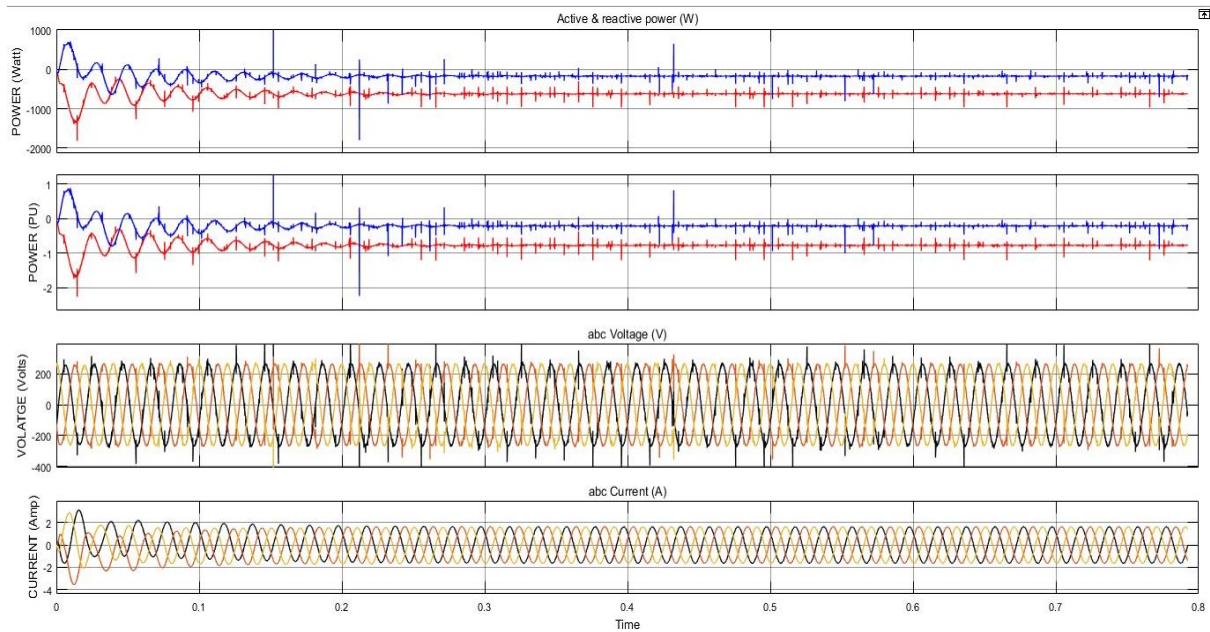


Fig 6.2.2 (a)

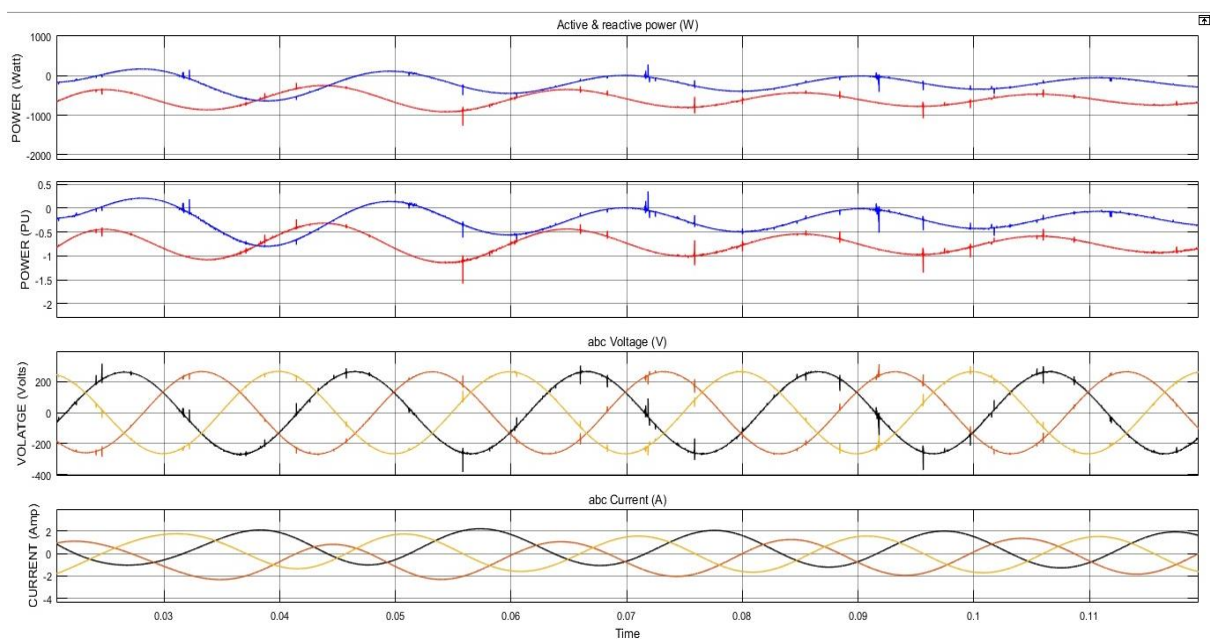


Fig 6.2.2 (b)

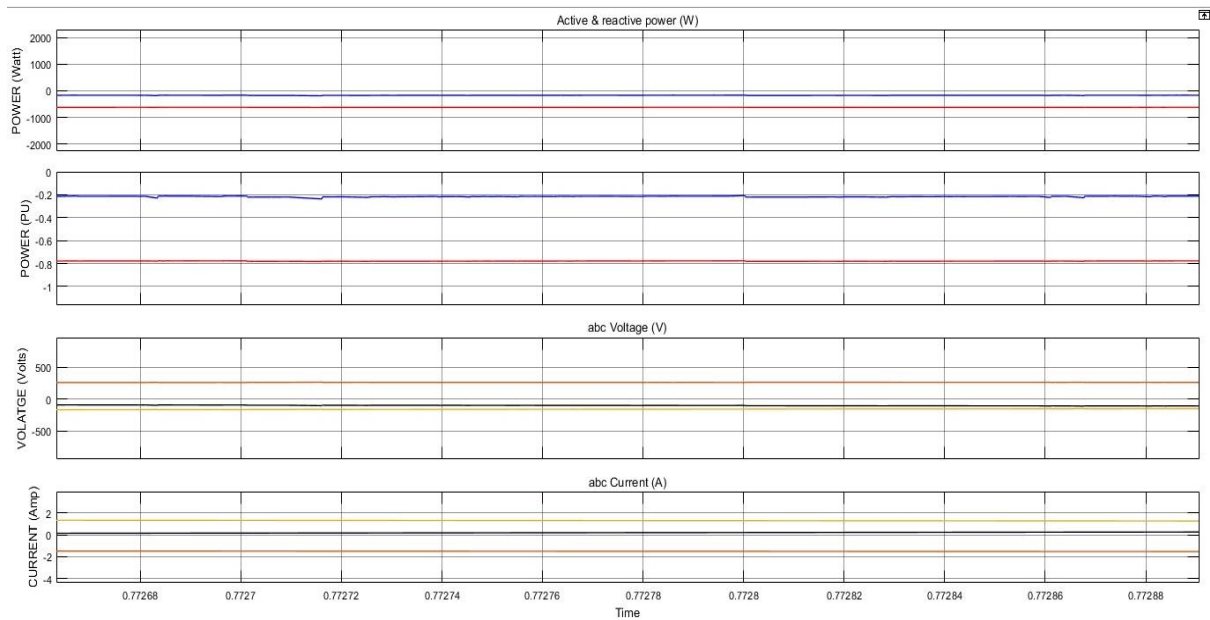


Fig 6.2.2 (c)

- The fig a shows the complete profile, fig b shows the initial transient value, and the fig c shows the final steady state value. The time is taken in seconds
- The red curve shows the active power and the blue curve shows the reactive power.
- The active power curve matches with the reference active power of 0.8 pu but there is some differences in reactive power.

6.3 OBSERVATIONS

For observations, we have only considered the sub-synchronous case. It has been verified experimentally that the results are almost same for super-synchronous case as well.

The reference values, in per unit, provided for calculation are as follows

CASE NO.	REFERENCE POWER (P_{s_ref})	ACTIVE	REFERENCE REACTIVE POWER (Q_{s_ref})
01	-0.2		-0.9
02	-0.3		-0.8
03	-0.4		-0.7
04	0.9		-0.3
05	-0.8		-0.4
06	-0.7		-0.3

The reference values and the actual values in per unit are as follows:

CASE NO.	REFERENCE ACTIVE POWER (P_{s_ref})	REFERENCE REACTIVE POWER (Q_{s_ref})	ACTUAL ACTIVE POWER (P_s)	ACTUAL REACTIVE POWER (Q_s)
01	0.2	0.9	0.19	0.7
02	0.3	0.8	0.28	0.61
03	0.4	0.7	0.4	0.62
04	0.9	0.3	0.92	0.11
05	0.8	0.4	0.79	0.21
06	0.7	0.3	0.69	0.13

The difference in reference and actual powers may be denoted as ∂_p and ∂_q , for active and reactive power respectively, then

CASE NO.	∂_p	∂_q
01	0.01	0.2
02	0.02	0.19
03	0.00	0.08
04	0.02	0.19
05	0.01	0.19
06	0.01	0.17

Analysing the data in graphical form:

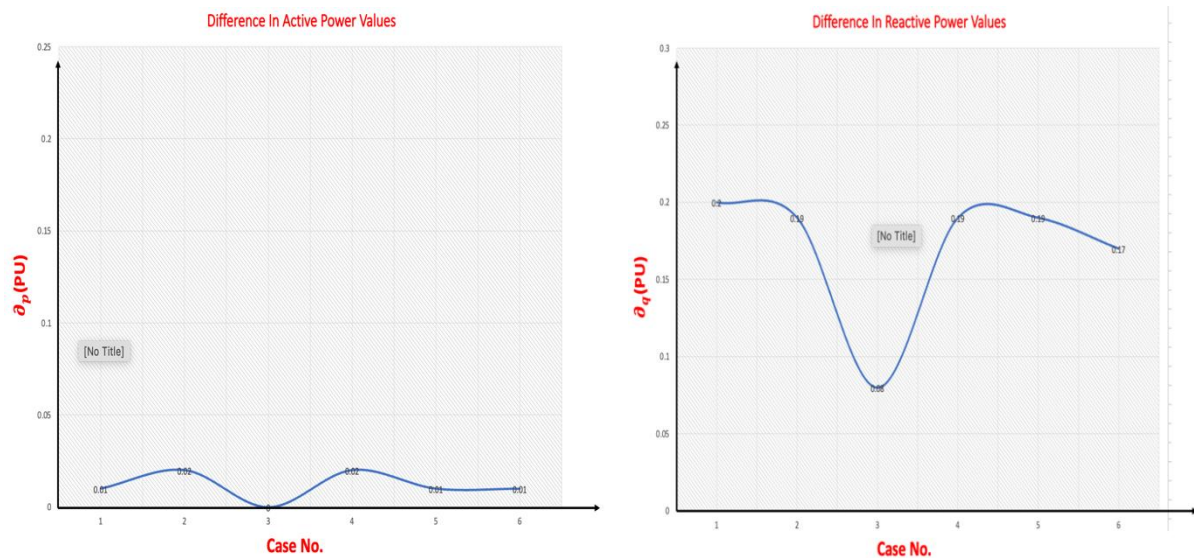


Fig. 6.3: Differences in active and reactive power with respect to its reference values

CHAPTER 7

CONCLUSIONS AND FUTURE WORK

7.1 CONCLUSIONS

From the active power curves for different values of reference active and reactive stator power, and by observing the actual values against the reference values, we can conclude that:

- The stator active power (P_s) is very close to the provided reference active power (P_{s_ref}) which suggests that the stator active power control by Rotor side Converter control is successful.
- The stator reactive power (Q_s), however differs from the reference value (Q_{s_ref}) by approximately 0.2 units pu, in most cases. We have varied Q_{s_ref} from -0.9 to -0.2 but throughout the range, we have observed the same nature, **barring one case**. This is for case no:3, for $Q_{s_ref} = 0.7 pu$
- By trial and error method, it is found that for $Q_{s_ref} \sim 0.6 \text{ to } 0.7 pu$ the variation of the actual power with the reference power is minimum.
- The other variations may be due to some constraints in the MATLAB modelling, which provides with scope for future work
- The curves for stator active, reactive power and stator 3 phase voltages shows some distortion from time to time, both during transient as well as steady state conditions. The nature of the 3 phase stator voltage is sinusoidal, with a phase shift of 120° between phases. But the distortion may be due to distortion in the signals, and also some constraints in MATLAB modelling.

7.2 SCOPE FOR FUTURE WORK

- The spikes in the power and voltage curve can be controlled by using some advanced kind of filters. Median filtering is a natural way to eliminate them. The effectiveness of the filter can be tested experimentally.
- The response obtained using other controllers can be compared with this work for further studies.
- Other changes can be made in the modelling to make Q_s close to Q_{s_ref} for a wide range of variation of Q_{s_ref}

7.3 REFERENCES

- [01] Zhe Chen, Josep M. Guerrero, and Frede Blaabjerg. "A Review of the State of the Art of Power Electronics for Wind Turbines" in IEEE Transactions on Power Electronics, VOL. 24, NO. 8, AUGUST 2009, DOI:10.1109/TPEL.2009.2017082
- [02] F. Blaabjerg, Z. Chen, and S. B. Kjaer, "Power electronics as efficient interface in dispersed power generation systems," IEEE Trans. Power Electron., vol. 19, no. 5, pp. 1184–1194, Sep. 2004.
- [03] Jamal A. Baroudi, Venkata Dinavahi, and Andrew M. Knight, "A review of power converter topologies for wind generators," Int. Journal of Renewable Energy, vol.32, no.14, pp.2369–2385, 2007
- [04] M.Y. Uctug, I. Eskandarzadeh and H. Ince, "Modelling and output power optimization of a wind turbine driven double output induction generator," Proc. IEEE Electric Power Applications, vol. 141, no. 2, pp. 33-38, Mar 1994.
- [05] A.Tapia, G. Tapia, J.X. Ostolaza and J.R. Saenz, "Modelling and control of a wind turbine driven doubly fed induction generator," IEEE Trans. Energy Conversion, vol. 18, no. 2. pp. 194 – 204, June 2003
- [06] D.Aouzellag , K.Ghedamsi, E.M.Berkouk "Power Control of a Variable Speed Wind Turbine Driving an DFIG" in RE&PQJ, Vol. 1, No.4, April 2006 DOI: 10.24084/repqj04.220
- [07] Badrul H. Chowdhury and Srinivas Chellapilla, "Double-fed induction generator control for variable speed wind power generation," Electric Power Systems Research, vol. 76, no. 9-10, pp. 786-800, June 2006.
- [08] M. Yamamoto and O. Motoyoshi, "Active and reactive power control for doubly fed wound rotor induction generator," IEEE Trans. Power Electronics, vol. 6, no. 4, pp. 624-629, Oct 1991
- [09] L. Xu and Y. Wang, "Dynamic modeling and control of DFIG-based wind turbines under unbalanced network conditions," IEEE Trans. Power Syst., vol. 22, No. 1, pp. 314–323, Feb. 2007.
- [10] Yongchang Zhang, Jian Jiao and Donglin Xu "Direct Power Control of Doubly Fed Induction Generator Using Extended Power Theory Under Unbalanced Network" in IEEE TRANSACTIONS ON POWER ELECTRONICS DOI: 10.1109/TPEL.2019.2906013
- [11]H. Akagi, Y. Kanazawa, and A. Nabae, "Instantaneous reactive power compensators comprising switching devices without energy storage components," IEEE Trans. Ind. Appl., vol. 20, no. 3, pp. 625–630, 1984.
- [12] A.V.Timbus, P.Rodriguez, R.Teodorescu, M.Liserre,andF.Blaabjerg, "Control strategies for distributed power generation systems operating on faulty grid," in Proc. IEEE Int Industrial Electronics Symp, vol. 2, 2006, pp. 1601–1607.

[13] Lei sun, Zengqiang Mi, Yang Yu, Tao Wu, Haifeng Tian, “ Active Power and Reactive Power Regulation Capacity Study of DFIG Wind Turbine” in IEEE 2009 International Conference.

[14] Sergei P, Andrea T, and Alerto T, “Power control of a doubly fed induction machine via output feedback,” Control Engineering Practice, vol. 12, pp. 41-57, Jan. 2004.

[15] F. Mazouz, S. Belkacem, Y. Harbouche, R. Abdessemed and S. Ouchen “Active and Reactive Power Control of a DFIG For Variable Speed Wind Energy Conversion” in Proceedings of the 6th International Conference on SuAB.1 Systems and Control, University of Batna 2, Batna, Algeria, May 7-9, 2017

[16] <https://www.linquip.com/blog/how-do-wind-turbine-generators-work/> last access on 25/06/2023

[17] Lectures of Prof (Dr.) S. S. Murthy, Department of Electrical Engineering, IIT Delhi, July 2018

[18] <https://www.explainthatstuff.com/windturbines.html>, last access on 25/06/2023

[19] <https://www.investindia.gov.in/sector/renewable-energy>, last access on 25/06/2023